



Si113-prodrugs selectively activated by plasmin against hepatocellular and ovarian carcinoma



Enrico Rango ^{a,1,2}, Lucia D'Antona ^{b,1}, Giulia Iovenitti ^a, Annalaura Brai ^a, Arianna Mancini ^a, Claudio Zamperini ^c, Claudia Immacolata Trivisani ^a, Stefano Marianelli ^a, Anna Lucia Fallacara ^a, Alessio Molinari ^a, Annarita Ciancusi ^d, Silvia Schenone ^d, Nicola Perrotti ^{b,**}, Elena Dreassi ^{a,*}, Maurizio Botta ^{a,c,e}

^a Dipartimento di Biotecnologie, Chimica e Farmacia, Università degli Studi di Siena, Via Aldo Moro 2, 53100, Siena, Italy

^b Dipartimento di Scienze della Salute, Università "Magna Graecia" di Catanzaro, Viale Europa, 88100, Catanzaro, Italy

^c Lead Discovery Siena S.r.l., Via Vittorio Alfieri 31, 53019, Castelnuovo Berardenga, Siena, Italy

^d Dipartimento di Farmacia, Università degli Studi di Genova, Viale Benedetto XV 3, Genoa, 16132, Italy

^e Sbarro Institute for Cancer Research and Molecular Medicine, Center for Biotechnology, College of Science and Technology Temple University, BioLife Science Building, Suite 333, 1900 North 12th Street, Philadelphia, PA, 19122, United States

ARTICLE INFO

Article history:

Received 18 March 2021

Received in revised form

1 June 2021

Accepted 13 June 2021

Available online 17 June 2021

Keywords:

Sgk1
Kinase inhibitors
HCC
Ovarian carcinoma
Prodrugs
Plasmin-activated prodrugs
Targeted therapy
ADME
Pharmacokinetic

ABSTRACT

Si113, a pyrazolo[3,4-*d*]pyrimidine derivative, gained more attention as an anticancer agent due to its potent anticancer activity on both *in vitro* and *in vivo* hepatocellular carcinomas (HCC) and ovarian carcinoma models. But the drawback is the low water solubility which prevents its further development.

In this context, we successfully overcame this limitation by synthesizing two novel prodrugs introducing the amino acid sequence D-Ala-Leu-Lys (TP). Moreover, TP sequence has a high affinity with plasmin, a protease recognized as overexpressed in many solid cancers, including HCC and ovarian carcinoma. The prodrugs were synthesized and fully characterized in terms of *in vitro* ADME properties, plasma stability and plasmin-induced release of the parent drug. The inhibitory activity against Sgk1 was evaluated and *in vitro* growth inhibition was evaluated on ovarian carcinoma and HCC cell lines in the presence and absence of human plasmin. *In vivo* pharmacokinetic properties and preliminary tissue distribution confirmed a better profile highlighting the importance of the prodrug approach. Finally, the prodrug antitumor efficacy was evaluated in an HCC xenografted murine model, where a significant reduction (around 90%) in tumor growth was observed. Treatment with ProSi113-TP in combination with paclitaxel in a paclitaxel-resistant ovarian carcinoma xenografted murine model, resulted in an impressive reduction of tumor volume greater than 95%. Our results revealed a promising activity of Si113 prodrugs and pave the way for their further development against resistant cancer.

© 2021 Elsevier Masson SAS. All rights reserved.

1. Introduction

Compound Si113 (Fig. 1a), a pyrazolo[3,4-*d*]pyrimidine derivative, has been identified as a potent inhibitor of Sgk1 [1,2] (serum and glucocorticoid-regulated kinase 1) which belongs to the serine/

threonine kinase family. In the last years, this protein gained more and more attention as a molecular target in oncology, being involved at different levels in the development and progression of different types of cancer [3], including breast [4,5], prostate [6], ovarian [7], non-small-cell lung cancer (NSCLC) [8], hepatocellular carcinoma (HCC) [9,10] and malignant glioma [11]. Sgk1 is activated by cAMP, insulin [12], growth factors [13,14], and steroids [15] and participates in a wide variety of pathways and mechanisms promoting tumor cell proliferation and conferring resistance to apoptosis. Sgk1 has been demonstrated to be an Akt-independent critical PI3K downstream effector [16,17], to regulate Ca²⁺-dependent tumor growth [18], through the control of potassium channels, to contribute cell survival, proliferation, and differentiation by

* Corresponding author.

** Corresponding author.

E-mail addresses: perrotti@unicz.it (N. Perrotti), elena.dreassi@unisi.it (E. Dreassi).

¹ Both authors contributed equally to this work.

² Present addresses: Dipartimento di Farmacia, Università degli Studi di Genova, Viale Benedetto XV 3, Genoa 16132, Italy.

Abbreviations			
Sgk1	Serum and Glucocorticoid-regulated Kinase 1	PAMPA	Parallel Artificial Membrane Permeability Assay
HCC	Hepatocellular Carcinoma	%MR	Membrane retention
TP	D-Ala-Leu-Lys tripeptide	DMSO	Dimethyl sulfoxide
SCLC	Non-small-cell lung cancer	MD	Molecular dynamic
MDM2	Mouse Double Minutes 2	PK	Pharmacokinetic
LK	Linker	TAX	Paclitaxel
EDC	1-Ethyl-3-(3dimethylaminopropyl)carbodiimide	ACN	Acetonitrile
DMAP	4-Dimethylaminopyridine	HLM	Human liver microsomes
TFA	Trifluoroacetic acid	DMEM	Dulbecco's Modified Eagle's Medium
LKTP	Linker-Tripeptide	FBS	Fetal Bovine Serum
ADME	Absorption distribution, metabolism, and excretion	I.P.	Intraperitoneal
		%ME	Matrix effect percentage
		%RE	Recovery percentage

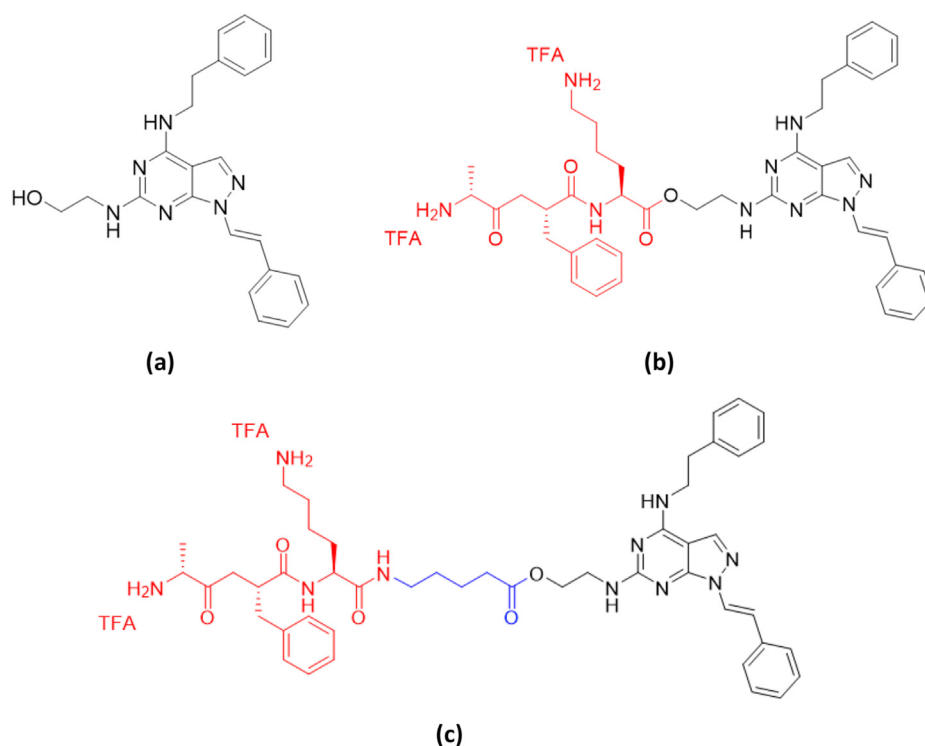


Fig. 1. Chemical structures of (a) Si113, (b) ProSi113-TP and (c) ProSi113-LKTP. (Black: parent drug Si113; Red: tripeptide sequence, TP; Blue: linker, LK; TFA: Trifluoroacetic acid).

phosphorylation of Mouse Double Minutes 2 (MDM2) [19]. In addition, Sgk1 is implicated in conferring resistance to chemo- and radiotherapy, affecting cellular sensitivity to taxol, by regulating the expression of RANBP1, which is also involved in the alteration of mitotic stability [20].

As a potent inhibitor of Sgk1 (IC_{50} value of 600 nmol/L) [1], Si113 was found to induce apoptosis and to reduce proliferation in different cancer cell lines, in which this protein is overexpressed/overactivated: RKO colorectal adenocarcinoma cells [2], MCF-7 breast cancer cells [2], A-172, (L1)PARI, ADF, and T98G glioblastoma multiforme cells [11], HepG2 and HuH-7 HCC cell lines [21], A2780 ovarian cancer cells [22], Ishikawa, HEC1B, and AN3CA endometrial cancer cell lines [23]. Furthermore, Si113 showed a good safety profile, being non-toxic on human fibroblast cells up to a concentration of 50 μ M [11].

In particular, the inhibition of Sgk1 by Si113 has been proved to strongly reduce HCC cellular viability, with a dramatic increase in apoptosis and altered cell cycle. In addition, Si113 was intraperitoneally administered at a dosage of 8 mg/kg in human HCC cell-xenografted mice, arresting cancer growth, inducing high levels of necrosis in tumor tissues, and synergizing with radiotherapy [21]. Moreover, in *in vitro* and *in vivo* preclinical models of ovarian cancer, Si113 inhibits tumor cell proliferation, synergizes with paclitaxel, and rescues paclitaxel sensitivity in resistant cells [22].

The aim of this work is the improvement of the efficacy and the benefits of the Si113 therapy in HCC and ovarian cancer, thanks to the application of a prodrug strategy, which allows for the activation of the parent drug locally at the tumor site. Indeed, most conventional chemotherapeutics are characterized by poor pharmacokinetic profiles and non-specific distribution in body tissues.

Accordingly, the development of rationally modified prodrugs can lead to the realization of targeted cancer therapy, avoiding off-target effects and enhancing the efficacy of conventional chemotherapy [24–26]. In this context, the aminoacidic sequence D-Ala-Leu-Lys (TP) has been selected, synthesized, and introduced as pro-moiety in the structure of Si113. Indeed, this tripeptide sequence has been proved to have a high affinity for a specific reactive site of plasmin [27], a protease recognized to be overexpressed in many tumors, including HCC [28] and ovarian cancer [29,30]. The plasmin system has a primary role in extracellular matrix degradation, tissue infiltration, angiogenesis, invasion, metastasis, and drug resistance [31]. Plasminogen is plasmin's inactive precursor, and it is locally converted by two types of high-affinity activators, urinary-type (uPA) and tissue-type (tPA). The conversion takes place when plasmin is bound to plasminogen-receptors, in its cell surface-associated form. This allows greater proteolytic activity and protection from inactivation for cell surface-associated plasmin [32]. Moreover, the selected amino acid sequence (TP) has been extensively studied for the design of doxorubicin prodrugs [33]. A clear improvement in the *in vivo* toxicity profile was achieved with the prodrugs approach, in contrast to the toxicity profile of the parent drug doxorubicin.

Being a tumor-related protease, plasmin has been already exploited in prodrug approaches, as a parent drug-releasing mediator [27,33,34]. We already explored the ability of the above-mentioned TP to target plasmin. TP was integrated as a targeting portion in a Si113-encapsulating liposomal system, which was successfully tested in *in vitro* models of HCC [35]. We now report the synthesis and preclinical characterization of plasmin-activated Si113 prodrugs, designed to be cleaved by plasmin, allowing for the release of the parent drug Si113 specifically at the tumor site. The alcohol on C-6 sidechain was chosen to readily synthesize the corresponding esters, avoiding protection and deprotection steps and ensuring rapid hydrolysis and thus a fast release of the parent drug. The amine in C-4 position was also evaluated, but the instability of carbamate was not compatible with TP deprotection steps, while the synthesis of the corresponding amide was not successful in acceptable yields (data not shown). All the prodrugs have been docked into plasmin pocket, to determine their binding modes (for details see supporting information). The first prodrug, named ProSi113-TP (Fig. 1b) is composed of the parent drug (black portion) and TP (red portion), connected by an ester link (where the cleavage takes place), while the second, ProSi113-LKTP (Fig. 1c), presents four carbon atoms introduced as linker (LK, blue portion) between drug Si113 and TP.

Si113-prodrugs have been characterized in terms of stability in polar media, human plasma, and human plasmin solution. In addition, Si113 and its prodrugs have been characterized for their water solubility, passive permeability, and metabolic stability. The *in vitro* antitumor activity was evaluated in HCC HepG2 and Huh-7, and human ovarian carcinoma A2780 cell lines. *In vivo* pharmacokinetic profile and preliminary 24 h biodistribution of Si113 and prodrugs were evaluated. Finally, their antitumor efficacy was evaluated in HCC and ovarian carcinoma mice models, also in combination with paclitaxel.

2. Results

2.1. Synthetic strategy

Si113-prodrugs have been synthesized starting from compounds Si113 and TP, which were previously synthesized and published by our group [35,36].

ProSi113-TP (**4**) was synthesized following the procedure reported in Scheme 1: TP (**1**) was activated for 30 min using EDC·HCl/

DMAP, then Si113 (**2**) was added, and the reaction mixture was stirred at room temperature for 72 h to obtain the intermediate **3**. Finally, the *N*-deprotection was performed with TFA affording the desired product ProSi113-TP (**4**) with a 99% yield.

For the synthesis of ProSi113-LKTP, the following steps have been performed. First, the ethyl 5-aminopentanoate hydrochloride (LK, **6**) was obtained starting from the 5-aminovaleic acid (**5**) and SOCl₂ in anhydrous EtOH, with a 99% yield (Scheme 2).

Then, LK (**6**) was coupled with TP (**1**) in presence of EDC·HCl/DMAP and subsequently *O*-deprotected using a 5% NaOH aqueous solution obtaining the derivative **8** (LKTP), (Scheme 3).

Finally, to synthesize ProSi113-LKTP the same synthetic approach used for Si113-TP was applied: LKTP (**8**) was coupled with Si113 (**2**) using EDC·HCl/DMAP as activating system to give the intermediate **9** protected. The latter was then reacted with TFA affording the desired product ProSi113-LKTP (**10**) with 99% yield (Scheme 4).

2.2. *In vitro* ADME assays

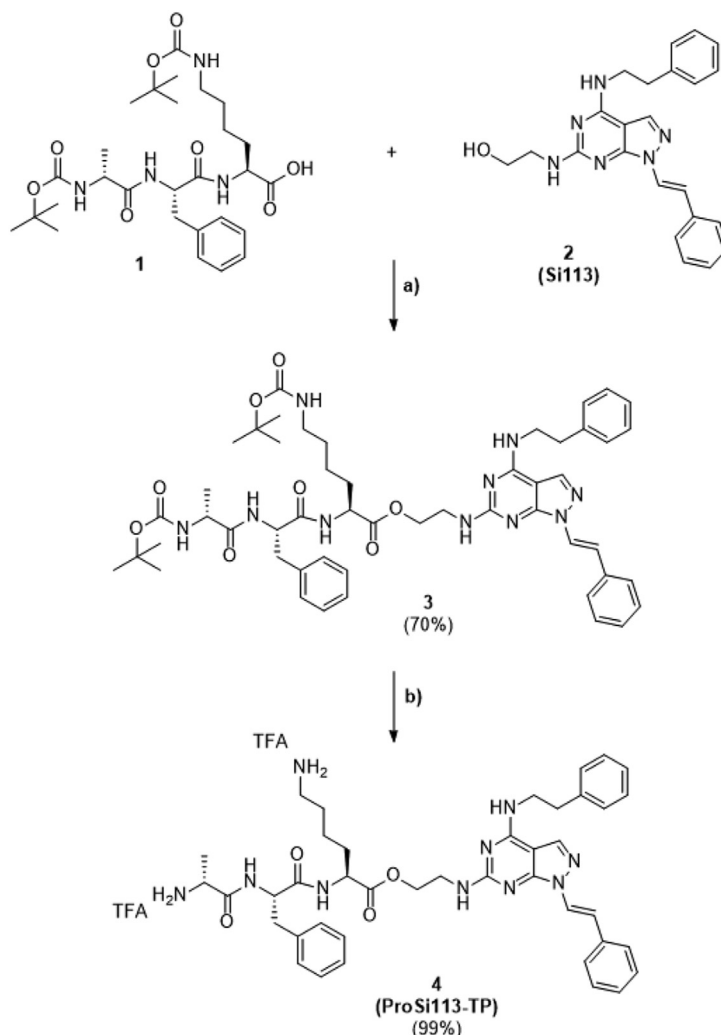
In vitro ADME properties were assessed, and the results are reported in the following Table 1. The ADME properties of Si113 (called **6c** in the manuscript) were previously determined and published in Radi et al. (2011) [36]. First, we have evaluated the thermodynamic water solubility of Si113 prodrugs. As expected, the water solubility has increased significantly for both prodrugs, which were 2500-times more soluble than the parent drug. After that, parallel artificial membrane permeability assay (PAMPA) was performed to evaluate the ability of these compounds to reach the cytoplasmic district in which our target enzyme is expressed. The results suggest for both prodrugs, a lower membrane permeability 10-fold less than the parental compound Si113 essentially due to their high degree of hydrophilicity. Moreover, both prodrugs provided good values of metabolic stability in human liver microsomes ($\geq 95\%$).

Finally, in order to evaluate the hydrolysis rate of prodrugs, stability tests were performed in polar solvents (DMSO, MeOH, and Tris buffer), human plasma, and human plasmin solution (Table 2). Prodrugs showed to be stable in polar solvents for more than 48 h. To verify the ability of ProSi113-TP and ProSi113-LKTP to release the corresponding parental drug Si113, both prodrugs were incubated at 37 °C in human plasma or plasmin solution for 24 h as described in the materials and methods section. ProSi113-TP, presenting only an ester as a hydrolyzable group, showed after 24 h a higher hydrolysis rate (65%) with half-life ($t_{1/2}$) value equal to 0.3 h in plasma and a lower hydrolysis rate in plasmin solution (40%) while maintaining a good half-life time ($t_{1/2} = 1.5$ h). On the other hand, ProSi113-LKTP, presenting two hydrolyzable sites, showed a plasma hydrolysis rate about of 35% and a higher hydrolysis rate (64%) in plasmin solution with comparable half-life values in human plasma and plasmin solution, equal to 4.6 and 3.1 h, respectively.

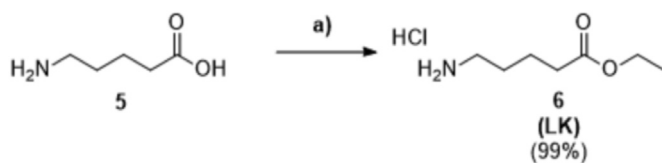
2.3. *In vitro* biological assay

2.3.1. *In vitro* evaluation of Sgk1 kinase inhibition

The interaction of Si113, ProSi113-TP and ProSi113-LKTP with Sgk1 was then tested in kinase assays. Sgk1 kinase activity was measured as radioactivity incorporated into specific target peptide (GRPRPTSSFAEGKK), in the presence of increasing drugs and prodrugs concentrations (0.6, 3, and 12.5 μ M) for 30 min. From the data obtained, Si113 is able to inhibit Sgk1 kinase activity in a dose-dependent manner showing inhibition of 75% as early as 0.6 μ M (increasing to more than 90% at 12.5 μ M). ProSi113-TP is able to significantly reduce Sgk1 activity by 80% only at a concentration of 12.5 μ M, while ProSi113-LKTP reaches to reduce activity by 73% at a



Scheme 1. Preparation of ProSi113-TP.



Scheme 2. Preparation of linker (LK).

concentration of 12.5 μM , both compared to the control. The difference between the two prodrugs is observed at lower concentrations, where already at 0.6 μM ProSi113-LKTP showed a reduction in enzyme activity of approximately 53% in contrast to ProSi113-TP which is only 18% (Fig. 2).

2.3.2. Inhibition of Sgk1 kinase activity in an intact cell environment

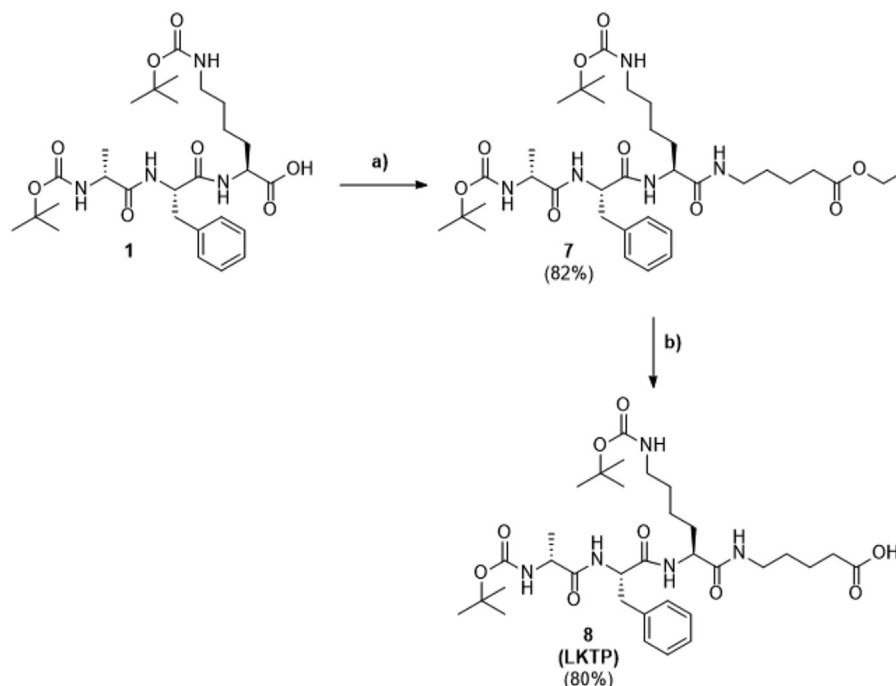
We investigated the effects of Si113, ProSi113-TP and ProSi113-LKTP on the enzymatic activity of endogenous Sgk1. HepG2 cells were incubated in the presence or absence of molecules (12.5 μM

for 12 h) and/or insulin (10^{-6} M) for the following 30 min. Cells were then lysed and Sgk1 protein was immunoprecipitated using an anti-Sgk1 antibody (#07–315, EMD Millipore). Sgk1 activity was then assayed in the immune complexes. Insulin increased significantly Sgk1 activity, as expected. Incubation of HepG2 cells in the presence of Si113 led approximately to a 35% inhibition of insulin-stimulated Sgk1 activity, thus suggesting that the molecule was able to permeate the cells and inhibit intracellular Sgk1 activity. Similarly, HepG2 cells incubation in the presence of ProSi113-TP and ProSi113-LKTP led approximately to a 40% inhibition of insulin-stimulated Sgk1 activity, suggesting that also the prodrugs, if hydrolyzed in an intact cellular environment, can permeate the membrane and inhibit the activity of Sgk1 (Fig. 3).

2.4. In silico studies

2.4.1. Molecular docking

To further confirm our results, docking studies have been performed on Si113, ProSi113-TP, and ProSi113-LKTP, using the previously published docking protocol (see supporting information for more details) [1]. The binding mode analysis of Si113 (Fig. 4a) shows that the alcoholic group of the compound interacts with the



Reagents and conditions: a) LK (6), EDC-HCl, dry CH_2Cl_2 , r.t., 16 h; b) NaOH 5%, r.t., 16 h.

Scheme 3. Preparation of LKTP.

backbone of Asp177 and Ile179 of Sgk1. The pyrazolo[3,4-*d*]pyrimidine core is inserted into a lipophilic area constituted by Val112, Ala125, Ile179, Leu229, and Thr239, while cation- π interactions are established between the phenyl group and Lys127. ProSi113-TP (Fig. 4b) shows a different orientation with respect to Si113 due to the steric hindrance of TP. The parent drug hydrophobically interacts with residues that constitute the binding site, without establishing other profitable interactions. Lys and Ala of TP establish hydrogen bond interactions with Glu226 and Leu229, respectively. The presence of a four-carbon atom linker in ProSi113-LKTP (Fig. 4c) allows the parent drug moiety to maintain the spatial orientation of Si113. The carbonyl group is involved in hydrogen bond interactions with the backbone of Ile179. Lys and Ala of TP are involved in hydrogen bond interactions with Glu183.

2.4.2. Molecular dynamics

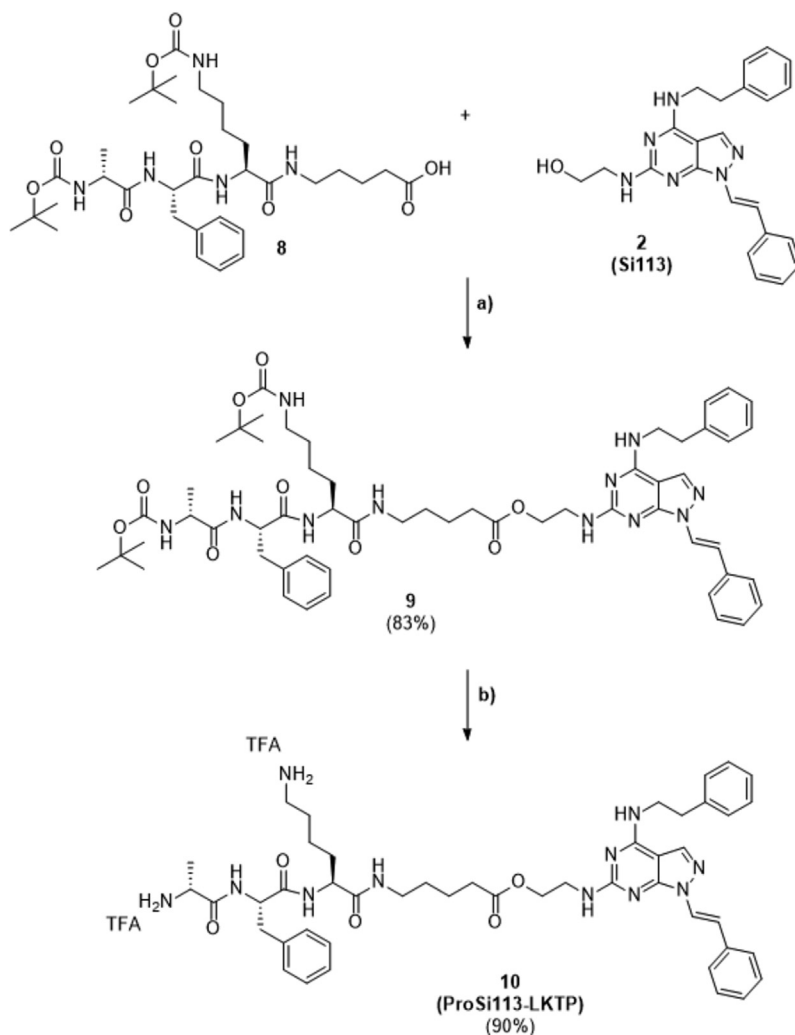
To further explore the stability and the dynamic behaviour of the compounds bound to Sgk1, 50 ns of molecular dynamics (MD) simulation were conducted using AMBER 16 software (see supporting information for more details). The analysis of the trajectories showed that Si113 is stably bound to the binding site of Sgk1 and is not subjected to great conformational changes. The Si113 RMSD plot shows a RMSD value which is stabilized around 3.5 Å (Fig. 5a). During the simulation, the -OH group is involved in hydrogen bond interactions with the backbone of Asp177 and with the side chain of Thr159. Other hydrogen bond interactions are established between the -NH group of the phenethylamine and the side chain of Thr239, and between the pyrazolo moiety and the side chain of Glu183. The MD simulation of ProSi113-TP shows that the compound is partially solvent-exposed and subjected to conformational changes that increase the RMSD values, oscillating around 4.5 Å and reaching a value of 6.5 Å (Fig. 5b). The pyrimidine moiety and the two amino groups form hydrogen bonds with water

molecules, and the -NH group of phenethylamine is also involved in H-bond interactions with the backbone of Ile179. During the simulation, TP interacts with Glu183, Glu226, Glu262, and Ile104. Finally, the analysis of the trajectory of ProSi113-LKTP shows that, after the assessment of the compound into the binding site, it stably interacts with amino acids that constitute the pocket (RMSD shows the increase of the RMSD values at the beginning of the simulation, Fig. 5c). The ester link forms long-lasting contacts with the backbone of Ile179, while the TP is involved in hydrogen bond interactions with Glu183, Glu226, and Ile179.

2.5. HCC

2.5.1. In vitro cytotoxicity assays

HepG2 and Huh-7 HCC cell lines were plated (see material and methods section). After 24 h, when cells were approximately 60% confluent, increasing concentration (0.1 μM , 1 μM , 10 μM , and 100 μM) of Si113, ProSi113-TP and ProSi113-LKTP were added, and cell viability was estimated after 24, 48, and 72 h (Table 3). In human HCC cell lines, Si113 yielded a significant dose-dependent reduction in the number of viable cells with IC_{50} values (after 72 h) of 3.15 and 0.58 μM on HepG2 and Huh-7 cell lines, respectively. Regarding prodrugs, on HepG2 cell line, ProSi113-TP and ProSi113-LKTP at 72 h showed IC_{50} values equal to 9.49 and 3.92 μM , respectively. On Huh-7, ProSi113-TP showed a slight reduction in cell viability with an IC_{50} value of 13.85 μM after 72 h. On the contrary, ProSi113-LKTP showed a significant reduction already after 24 h to reach an IC_{50} value equal to 0.74 μM after 72 h. In addition, we performed cytotoxicity tests in the presence of plasmin (0.2 U/well, final concentration) to assess whether the activity of the prodrugs increases due to the hydrolytic action of plasmin. In this regard, ProSi113-TP showed increased cytotoxicity after 24 h with up to 2 times higher reduction in cell viability for



Reagents and conditions: a) EDC·HCl, dry CH₂Cl₂, r.t., 16 h; b) TFA, dry CH₂Cl₂ dry, r.t., 3h.

Scheme 4. Preparation of ProSi113-LKTP.

Table 1

In vitro ADME assays of Si113 and its prodrugs.

Assays	Measurement Units	Si113	ProSi113-TP	ProSi113-LKTP
Water Solubility	µg/mL	0.4	>1000	>1000
PAMPA (%MR ^a)	10 ⁻⁶ cm/s (%)	2.6 (86.2)	0.2 (0)	0.2 (0)
Metabolic Stability ^b	%	84	≥95	≥95

^a Membrane Retention (%MR) expressed as percentage of compound unable to reach the acceptor compartment.

^b Expressed as percentage of unmodified compound.

Table 2

Stability assays of prodrugs in polar media, human plasma and human plasmin solution.

Stability in:	Unit	ProSi113-TP	ProSi113-LKTP
DMSO, MeOH and Tris Buffer	h	>48	>48
Human Plasma	% Hydrolysis (t _{1/2} ^a , h)	65 (0.3)	35 (4.6)
Human Plasmin solution		40 (1.5)	64 (3.1)

^a Half-life expressed as the amount of time it takes before half of the prodrugs are hydrolyzed.

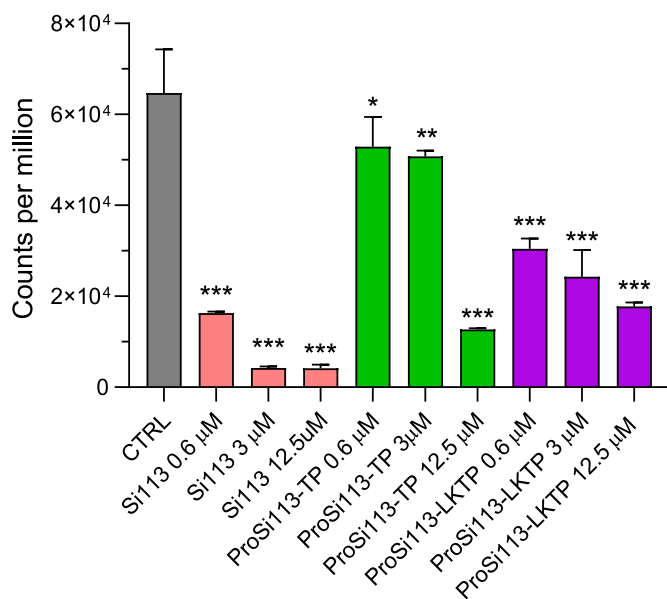


Fig. 2. Sgk1 kinase inhibition activity of Si113, ProSi113-TP and ProSi113-LKTP in enzymatic assay. A Bonferroni's one-way multiple comparisons test (ANOVA) was performed to test the significance of the observed differences. *indicates statistically significant differences between each treatment vs CTRL (* $p < 0.05$, ** $p < 0.01$ and *** $p < 0.001$).

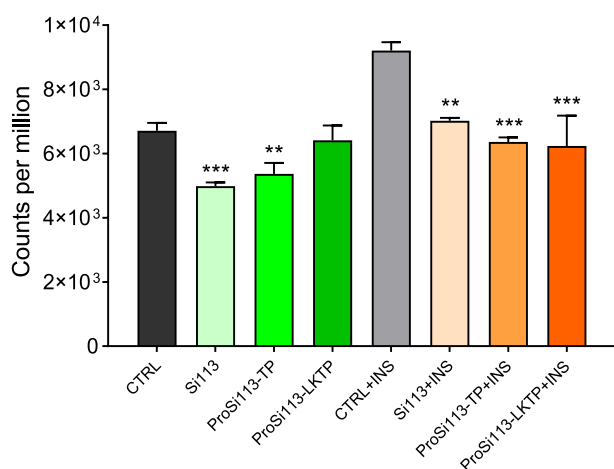


Fig. 3. Inhibition of Sgk1 kinase isolated from cell lysates. A Bonferroni's one-way multiple comparisons test (ANOVA) was performed to test the significance of the observed differences. *indicates statistically significant differences between each treatment vs its respective CTRL (** $p < 0.01$ and *** $p < 0.001$).

both HCC cell lines whereas, ProSi113-LKTP showed increased cytotoxicity against Hep-G2 cell line with up to 4 times higher reduction in cell viability.

2.5.2. In vivo administration of Si113 and prodrugs in male healthy mice

Preliminary pharmacokinetic and biodistribution tests were performed. For this purpose, plasma and tissue distribution profile of Si113 and both prodrugs were quantified after intraperitoneal administration. Si113, previously dissolved in DMSO [37], was administered as a single dose of 9.5 mg/kg in a final volume of 50 μ L. Both prodrugs were solubilized in saline solution at a single dose of 21 mg/kg in a final volume of 100 μ L. After treatments, mice were sacrificed, and blood and organs were collected. The

concentration of the compounds was determined by HPLC-MS/MS analysis. Table S1 (supporting information) shows the recovery and matrix effect data, which suggests that the developed analysis method could be successfully applied to the pharmacokinetic and biodistribution studies. The plasma concentration-time curves (expressed as nmol of compound/mL of plasma) of Si113 and its prodrugs are reported in Fig. 6, while the corresponding PK parameters are shown in Table 5.

Following intraperitoneal administration, Si113 was rapidly detected after 0.5 h (T_{max}) with a C_{max} of 46.27 nmol/mL while the observed C_{max} for ProSi113-TP and ProSi113-LKTP after 0.25 h were 8.09 and 2.66 nmol/mL, respectively. It is interesting to note how Si113 derived from the hydrolysis of ProSi113-LKTP reaches a C_{max} value of 21.31 nmol/mL after 1.50 h. In contrast, the Si113 derived from ProSi113-TP showed a 5-fold lower C_{max} value compared with the Si113 derived from ProSi113-LKTP (Table 5). However, ProSi113-TP showed an AUC_{0-24h} value almost 4-fold higher than ProSi113-LKTP. Regarding the AUC_{0-24h} values of Si113 resulting from the hydrolysis of each prodrug, Si113 released from ProSi113-LKTP showed an AUC_{0-24h} 6-fold higher than Si113 released from ProSi113-TP and the same trend is true for the parent drug Si113. The plasma half-life ($t_{1/2}$) and MRT values remain approximately in the same range after treatment with ProSi113-TP ($t_{1/2}$: 15.30 h, MRT: 18.41 h) and ProSi113-LKTP ($t_{1/2}$: 21.82 h, MRT: 31.55 h). On the contrary, Si113 showed a $t_{1/2}$ and MRT values of 2.73 h and 1.13 h respectively, while Si113 deriving from the hydrolysis of prodrugs showed for Si113 released by ProSi113-TP a two-fold higher half-life value ($t_{1/2}$: 4.13 h) compared to Si113 released by ProSi113-LKTP ($t_{1/2}$: 2.08 h). The same results were observed for the MRT values.

Si113 and its prodrugs were detected in all tissues collected from mice treated and sacrificed after 24 h (Fig. 7). ProSi113-LKTP showed higher tissue concentrations than Si113 and ProSi113-TP in all organs analyzed. In particular, in the hepatic tissue, for ProSi113-LKTP, it has been detected a concentration (11.05 nmol/g), almost 14-fold higher than that recorded for ProSi113-TP (0.81 nmol/g) and the same trend has also been observed for the drug released from prodrugs. The tissue concentration of Si113 resulting from ProSi113-LKTP (1.72 nmol/g) was almost 3-fold higher than that obtained from the hydrolysis of ProSi113-TP (0.65 nmol/g). On the other hand, the tissue concentrations of parent drug Si113 were comparable to those of Si113 released by ProSi113-LKTP hydrolysis. The same trend was also observed in renal tissue, where ProSi113-LKTP showed a higher tissue concentration (3.01 nmol/g) than ProSi113-TP (1.77 nmol/g), while similar Si113 levels for both parent drug and the drug derived by prodrugs hydrolysis were observed.

2.5.3. Human hepatocellular carcinoma xenograft mice model

HepG2 cells (2.5×10^6) were implanted in the flanks of nude female mice for *in vivo* treatment with vehicle alone, Si113, ProSi113-TP and ProSi113-LKTP at a dosage of 9.5 mg/kg/day for Si113 and 21 mg/kg/day for both prodrugs. Twenty mice were used, randomly subdivided into four batches. Treatment started when tumor volume reached 100 mm³, as assessed by manual caliper measurement. The drugs (or vehicle) were administered daily, and tumor growth was monitored every 7 days. Mice were sacrificed on day 21. Tumors were then excised and weighed. An impressive and significant reduction in tumor growth was recorded in all treated batches compared to controls (Fig. 8a). Measurements of the tumor weights further confirmed the effectiveness of the treatment (Fig. 8b) showing a significant reduction in mean tumor mass weight of approximately 93 and 87% for ProSi113-TP and ProSi113-LKTP treatments, respectively.

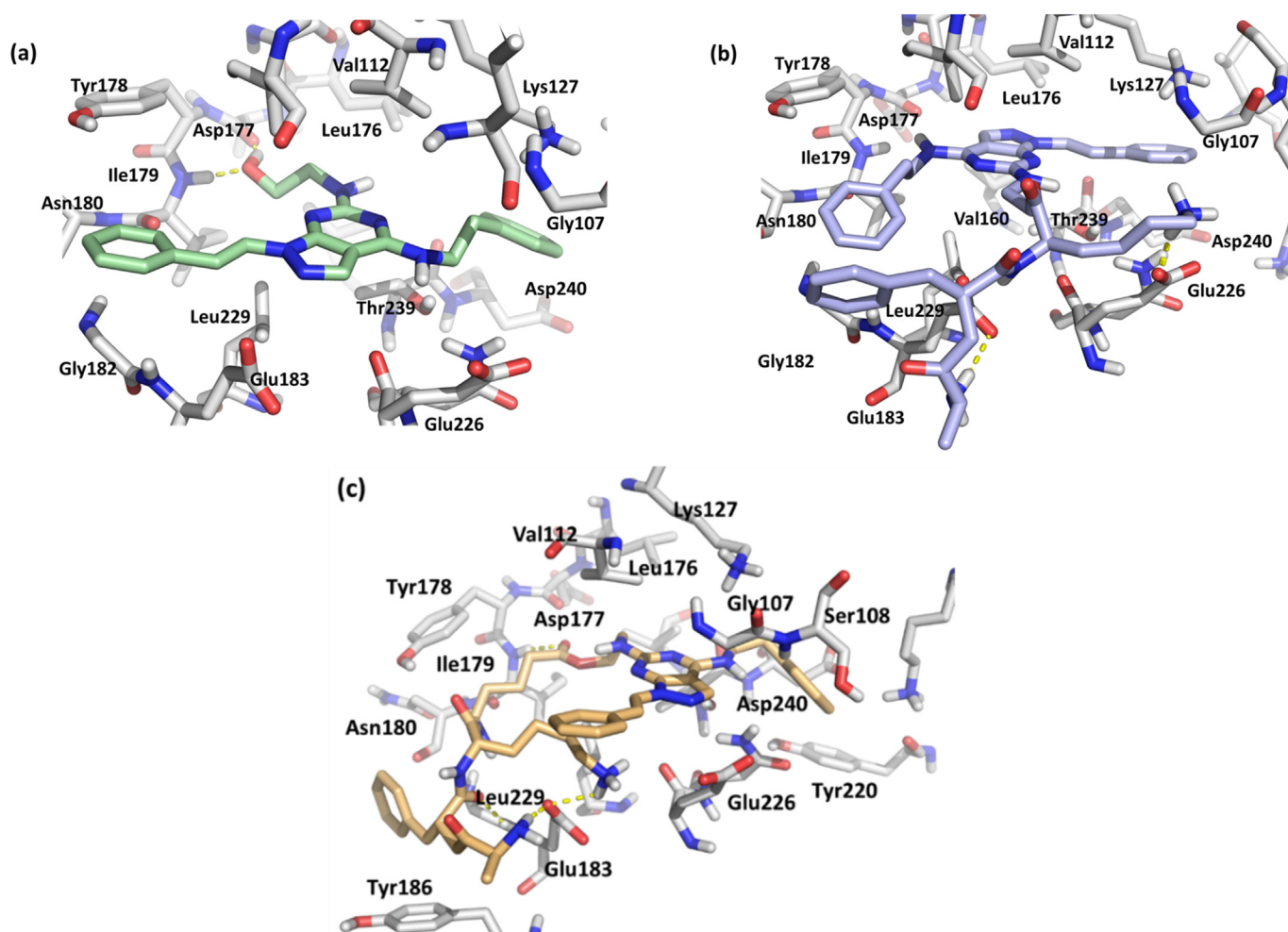


Fig. 4. Binding mode of (a) Si113 (green), (b) ProSi113-TP (blue) and (c) ProSi113-LKTP (orange) to the ATP binding pocket of Sgk1 (PDB ID: 3HDN).

2.6. Ovarian carcinoma

2.6.1. *In vitro* cytotoxicity assays

Preliminary cytotoxicity tests have been performed against A2780 ovarian cancer cell line. In recent work, D'Antona et al. (2019) [22] evaluated the activity of the Si113 inhibitor on ovarian cancer, indicating that it has the ability to inhibit cell proliferation, enhance the effects of paclitaxel-based chemotherapy and counteract the development of paclitaxel resistance and restore paclitaxel sensitivity in resistant A2780 ovarian cancer cells. In addition, *in vivo* preclinical studies on a xenograft model of nude mice implanted with paclitaxel-resistant human ovarian cancer cells have shown that the Si113 inhibitor has a synergistic action with paclitaxel in the treatment of xenografted ovarian cancer cells. For this reason, given the results obtained in this type of cancer, the cytotoxicity profile of prodrugs towards this type of cancer has been evaluated. Table 4 shows that Si113 yielded a significant dose-dependent reduction in the number of viable cells with IC_{50} values, after 72 h of 3.47 μ M. Similarly, prodrugs showed comparable cytotoxicity profiles with IC_{50} values (after 72 h) equal to 5.14 and 7.10 μ M for ProSi113-TP and ProSi113-LKTP, respectively. On the contrary, only ProSi113-TP showed an increased cytotoxicity profile up to 2 times higher in presence of plasmin with an IC_{50} value of 26.05 μ M.

2.6.2. Preliminary tissue distribution in nude female mice

Preliminary plasma and tissues concentrations profile was performed in two groups of nude female mice (Fig. 9a: A2780-

xenografted mice and Fig. 9b: non-xenografted mice) at 24 h after treatment with Si113 (9.5 mg/kg) and ProSi113-TP (21 mg/kg). Comparable plasma levels were detected in xenografted mice group with a higher concentration of Si113 resulting from the hydrolysis of ProSi113-TP (0.51 nmol/mL) than the parent compound (0.20 nmol/mL). The same trend was observed in the non-xenografted group with an almost two-fold lower plasma concentration almost two-fold lower for both the parental Si113 and the ProSi113-TP derived Si113 compared with the plasma levels observed in the A2780-xenografted mice group. Moreover, ProSi113-TP shows higher tissue concentrations than the parental drug in all organs examined. Interestingly the concentrations of ProSi113-TP detected in the tumor mass (5.69 nmol/g) were higher than the concentrations of Si113 released from the hydrolysis of ProSi113-TP (1.26 nmol/g). In contrast, the parental drug Si113 showed a tissue concentration (2.20 nmol/g) lower than its prodrug (Fig. 9a). The same is observed in ovarian tissue where Pro-Si113-TP showed a tissue concentration 2-fold higher than Si113 (4.11 and 1.89 nmol/g, respectively) and the same trend is detected in the ovaries of non-xenografted mice (Fig. 9b). Whereas comparable tissue concentrations of Si113, which was obtained after hydrolysis of ProSi113-TP, were observed in the ovaries of both animal groups (1.25–1.26 nmol/mL).

2.6.3. Ovarian carcinoma xenograft mice model

Based on the *in vitro* studies, we generated xenografts for *in vivo* experiments by implanting 2.5×10^6 paclitaxel-resistant A2780TC

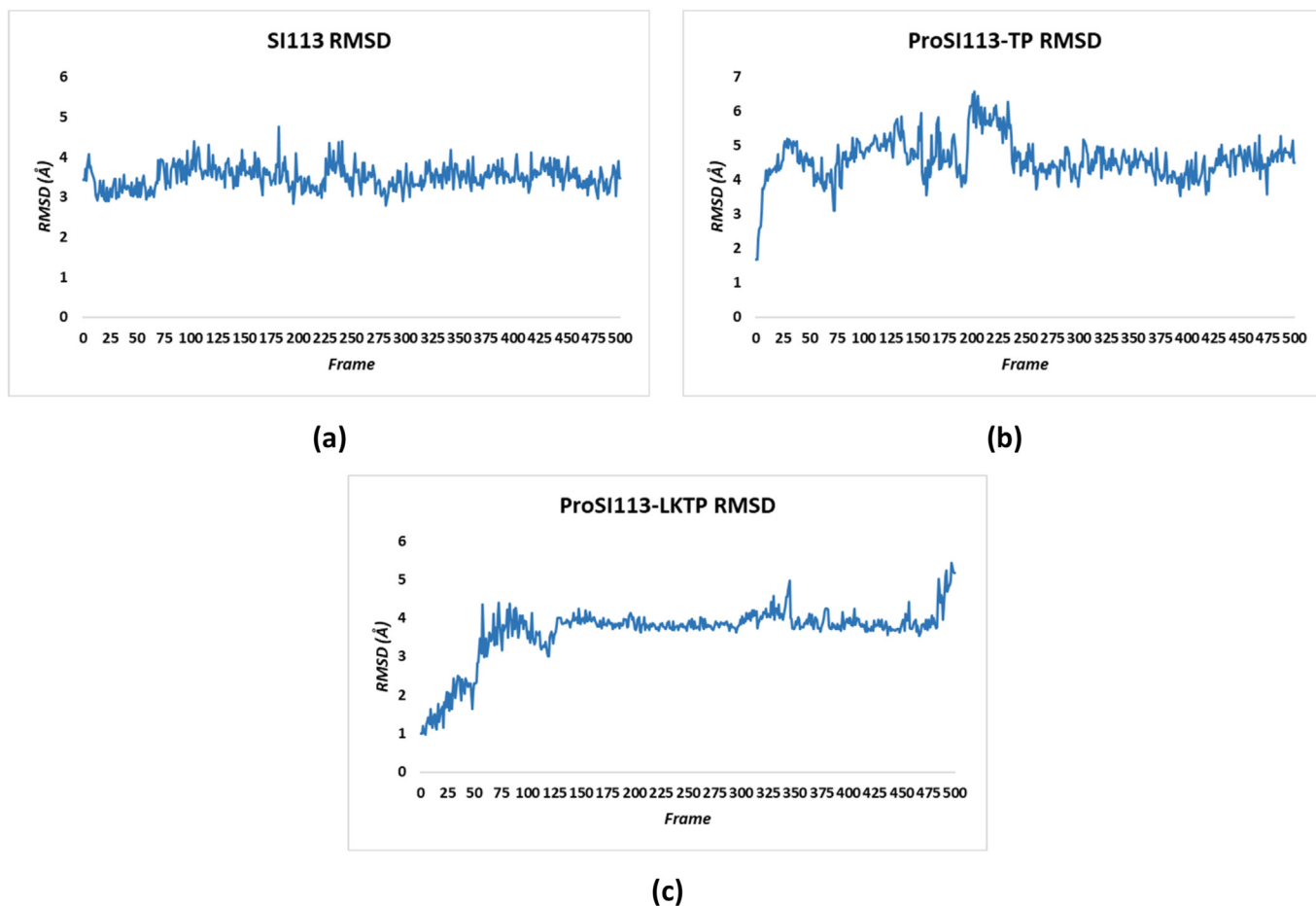


Fig. 5. RMSD plot of Si113, ProSi113-TP and ProSi113-LKTP. The line indicates the ligand fluctuation. (a) The Si113 RMSD plot shows a RMSD value which is stabilized around 3.5 Å. (b) The ProSi113-TP RMSD plot is characterised by values that oscillate around 4.5 Å and that reaches the value of 6.5 Å. The variations in the RMSD values are caused by conformational variation of the molecule, that is partially exposed to the solvent. (c) The ProSi113-LKTP RMSD shows the increase of the RMSD values at the beginning of the simulation. After the assessment of the compound into the binding site, it stably interacts with the amino acids that constitute the binding site.

Table 3

In vitro cytotoxicity assays of Si113 and both prodrugs against HepG2 and Huh-7 HCC cell lines.

Cell lines	Si113	ProSi113-TP	ProSi113-LKTP
HepG2		IC ₅₀ ^a (μM ± S.D.)	
24 h	15.87 ± 1.27	12.10 ± 1.32	14.69 ± 1.37
48 h	8.29 ± 0.54	9.49 ± 0.87	5.63 ± 0.40
72 h	3.15 ± 0.08	4.40 ± 0.39	3.92 ± 0.12
24 h + plasmin		6.75 ± 0.32	3.60 ± 0.07
Huh-7		IC ₅₀ ^a (μM ± S.D.)	
24 h	2.05 ± 0.12	>100	6.83 ± 0.37
48 h	1.88 ± 0.07	35.66 ± 2.62	1.58 ± 0.05
72 h	0.58 ± 0.03	13.85 ± 1.19	0.74 ± 0.03
24 h + plasmin		46.27 ± 2.17	6.72 ± 0.72

^a IC₅₀ was evaluated as dose-response inhibition of MTT assay. Data are means ± S.D. of three independent experiments each done in triplicate.

cells into the flanks of nude mice. Thirty xenografted mice were randomly divided into four experimental groups: I) treatment with the drug vehicle, II) treatment with Paclitaxel (TAX) at a dosage of 5 mg/kg, III) treatment with ProSi113-TP (21 mg/kg) and IV) treatment with ProSi113-TP in combination with Paclitaxel at the same dosages reported above respectively. The treatments were started 72 h after cell implantation, and the drugs (or vehicles) were administered five days per week. The tumor volumes were measured every 7 days for 21 days, as indicated in the Methods

section, and the mice were sacrificed on day 21. Tumors were excised, weighed and immediately frozen in liquid nitrogen. As expected, based on the known chemoresistance of A2780TC cells, Paclitaxel treatment did not affect tumor growth. As previously published in D'Antona L. et al. (2019) [22] and here reported for comparison with ProSi113-TP, the mice group treated with Si113 showed a significant reduction in tumor volume on day 21 compared with the control group, and a more substantial effect was observed in the mice treated with Si113 in combination with Paclitaxel (Fig. 10a [22]). The mice group treated with ProSi113-TP alone does not show a significant reduction compared with paclitaxel treatment alone but showed a substantial reduction (>95%) of tumor volume when used in combination with paclitaxel (Fig. 10c). Measurements of the tumor weights further confirmed the effectiveness of the treatment (Fig. 10b [22] and 10c).

3. Materials and methods

3.1. Synthesis and characterization of compounds

Compounds Si113 and TP were previously synthesized and published by our group [35,38].

All commercially available chemicals were used as purchased from Sigma Aldrich. CH₂Cl₂ was dried over sodium hydride, while MeOH and EtOH were dried over magnesium and iodine as indicator. Anhydrous reactions were run under a positive pressure of

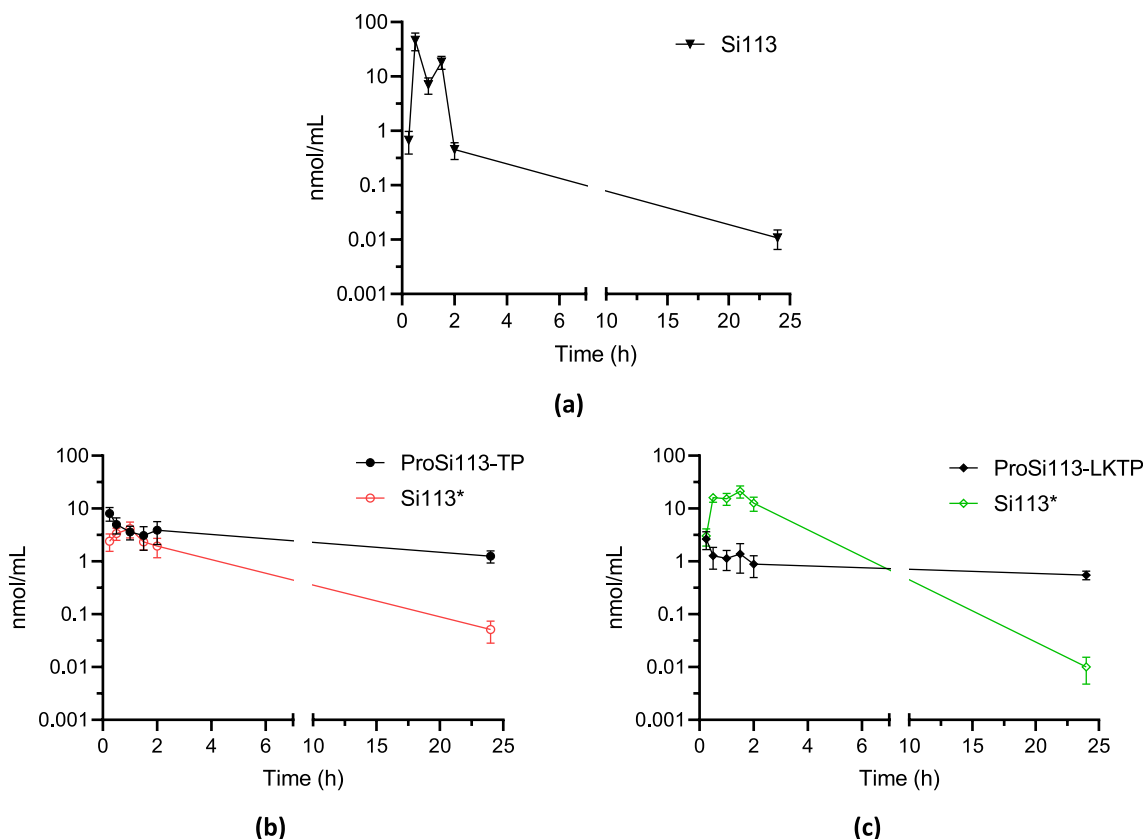


Fig. 6. Plasma concentration-time curves (mean \pm S.E.M., $n = 3$) after intraperitoneal administration of (a) Si113 9.5 mg/kg, (b) ProSi113-TP 21 mg/kg and (c) ProSi113-LKTP 21 mg/kg. The plasma concentrations in the y-axis are expressed as \log_{10} scale. *Si113 marked with asterisk represents the amount of drug detected deriving from the hydrolysis of prodrugs.

Table 4

In vitro cytotoxicity assays of Si113 and ProSi113-TP against A2780 ovarian carcinoma cell line.

Cell line	Si113	ProSi113-TP	ProSi113-LKTP
A2780		IC ₅₀ ^a ($\mu\text{M} \pm \text{S.D.}$)	
24 h	25.64 \pm 1.72	41.58 \pm 3.36	21.43 \pm 0.97
48 h	4.56 \pm 0.27	11.30 \pm 2.49	22.06 \pm 1.07
72 h	3.47 \pm 0.19	5.14 \pm 0.34	7.10 \pm 0.41
24 h + plasmin		26.05 \pm 1.55	21.60 \pm 1.56

^a IC₅₀ was evaluated as dose-response inhibition of MTT assay. Data are means \pm S.D. of three independent experiments each done in triplicate.

dry N₂. TLC was carried out using Merck TLC silica gel 60 F₂₅₄. Chromatographic purifications were performed on columns packed with Merck silica gel 60, 23–400 mesh, for flash technique. ¹H NMR and ¹³C NMR spectra were recorded at 400 MHz on a NMR Bruker Advance DPX400. Chemical shifts are reported relative to tetramethylsilane at 0.00 ppm.

Mass spectra (MS) data were obtained using an Agilent 1100 LC/MSD VL system (G1946C) with a 0.4 mL/min flow rate using a binary solvent system of 95/5 = MeOH/H₂O. UV detection was monitored at 254 nm. MS were acquired in positive and negative mode scanning over the mass range 100–1500 *m/z*. The following ion source parameters were used: drying gas flow, 9 mL/min; nebulizer pressure, 40 psi; drying gas temperature, 350 °C.

All target compounds possessed a purity of $\geq 95\%$ verified by UV/LC-MS method, as reported in UV/LC-MS methods section.

3.2. In vitro ADME assays

3.2.1. Chemicals

All solvents and reagents were from Sigma-Aldrich Srl (Milan, Italy). Dodecane was purchased from Fluka (Milan, Italy). Pooled male donors 20 mg/mL HLM were from BD Gentest-Biosciences (San Jose, California). Milli-Q quality water (Millipore, Milford, MA, USA) was used. Hydrophobic filter plates (MultiScreen-IP, clear plates, 0.45 μm diameter pore size), 96-well microplates, and 96-well UV-transparent microplates were obtained from Millipore (Bedford, MA, USA).

3.2.2. UV/LC-MS methods

LC analyses for water solubility, blood samples and organs collected were performed by LC-MS/MS system consisted of a Varian apparatus (Varian Inc) including a vacuum solvent degassing unit, two pumps (212-LC), a Triple Quadrupole MSD (Mod. 320-LC) mass spectrometer with ES interface and Varian MS Workstation System Control Vers. 6.9 software. Chromatographic separation was obtained using a Pursuit C18 column (50 \times 2.0 mm) (Varian) with 3 μm particle size and gradient elution with a binary solution; (eluent A: ACN, eluent B: Water, both eluents were acidified with formic acid 0.1% v/v). The analysis started with 5% of A (from $t = 0$ to $t = 3$ min), then A was increased to 95% (from $t = 3$ to $t = 12$ min), then kept at 95% (from $t = 12$ to $t = 20$ min) and finally return to 5% of eluent A in 1.0 min. The flow rate was 0.2 mL/min and injection volumes were 5 μL . The instrument operated in positive mode and parameters were: detector 1850 V, drying gas

Table 5
Plasma pharmacokinetic parameters of Si113 and its prodrugs evaluated using a non-compartment model.^a

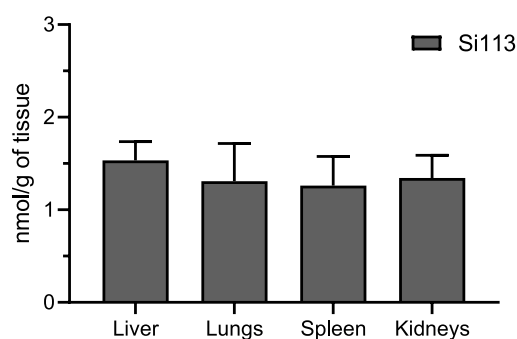
Parameters (Unit)	Plasma Pharmacokinetic Parameters ^a				
	9.5 mg/kg		21 mg/kg		
	Si113	ProSi113-TP	Si113 ⁱ	ProSi113-LKTP	Si113 ⁱ
$t_{1/2}$ ^b (h)	2.73	15.30	4.13	21.82	2.08
T_{max} ^c (h)	0.5	0.25	1.00	0.25	1.50
C_{max} ^d (nmol/mL)	46.27	8.09	4.16	2.66	21.31
$AUC_{0 \rightarrow 24h}$ ^e (nmol/mL·h)	35.48	64.58	27.65	18.41	167.46
$AUC_{0 \rightarrow \infty}$ ^e (nmol/mL·h)	35.52	92.26	27.95	35.71	167.49
$MRT_{0 \rightarrow \infty}$ ^f (h)	1.13	18.41	2.55	31.55	1.88
V_z/F^g ((mg/kg)/(nmol/mL))	1.05	5.02	4.48	18.51	0.38
CL/F^h ((mg/kg)/(nmol/mL/h))	0.28	0.23	0.75	0.59	0.13

^a Calculated with PKSolver.^b $t_{1/2}$: half-life.^c T_{max} : time of maximum concentration observed.^d C_{max} : maximum concentration observed.^e AUC: area under the curve.^f MRT: mean residence time.^g V_z : volume of distribution.^h CL: clearance.ⁱ Si113 marked with an asterisk represents the drug deriving from the hydrolysis of each prodrug.

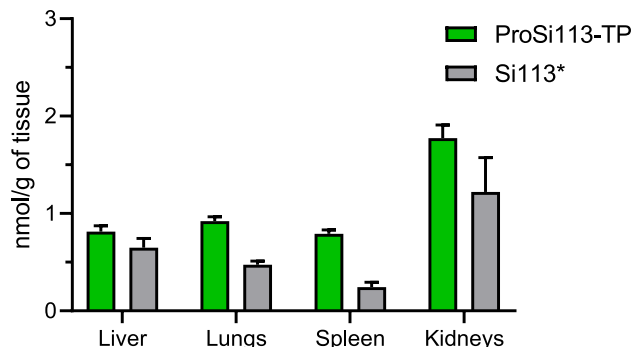
pressure 25.0 psi, desolvation temperature 300.0 °C, nebulizing gas 45.0 psi, needle 5000 V and shield 600 V. Nitrogen was used as nebulizer gas and drying gas. Collision induced dissociation was performed using Argon as the collision gas at a pressure of 1.8 mTorr in the collision cell. The transitions as well as the capillary voltage and the collision energy used are appropriated for each

tested compound. Quantification of the single compound was made by comparison with appropriate calibration curves realized with standard solutions in methanol.

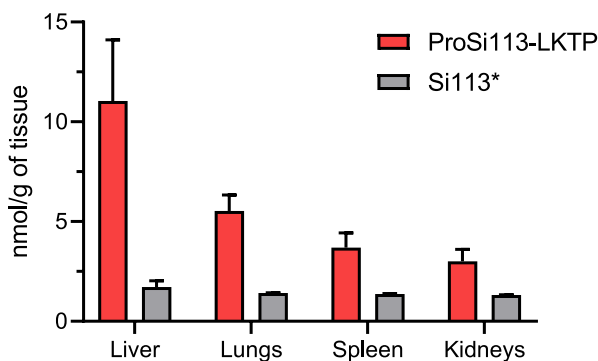
LC analyses of PAMPA, Metabolic Stability and Stability Tests (in DMSO, MeOH, Tris-buffer, human plasma and human plasmin solution) were performed by UV/LC-MS with an Agilent 1100 LC/MSD



(a)



(b)



(c)

Fig. 7. Tissue distribution concentration profile (mean \pm S.E.M., $n = 3$) in male healthy mice at 24 h after treatment with (a) Si113 9.5 mg/kg, (b) ProSi113-TP 21 mg/kg and (c) ProSi113-LKTP 21 mg/kg *Si113 marked with an asterisk represents the amount of drug detected deriving from the hydrolysis of prodrugs.

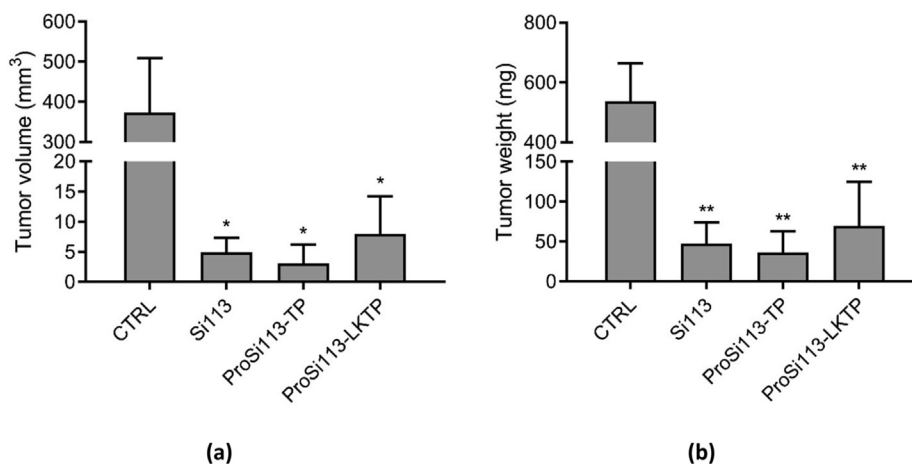


Fig. 8. HCC *in vivo* efficacy on HepG2-xenografted mice model. (a) tumor volume and (b) tumor weight (mean \pm S.D., $n = 5$). A Bonferroni's one-way multiple comparisons test (ANOVA) was performed to test the significance of the observed differences. *indicates statistically significant differences between each treatment vs CTRL (* $p < 0.05$, ** $p < 0.01$).

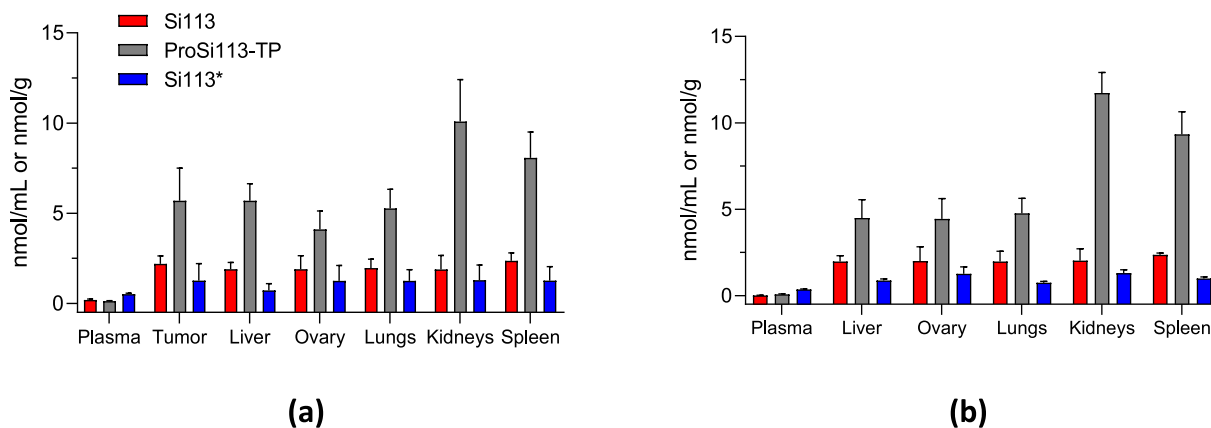


Fig. 9. Plasma and tissue concentrations (mean \pm S.E.M., $n = 2$, plasma: nmol/mL; tissues: nmol/g) profile at 24 h after treatment with Si113 in red, ProSi113-TP in grey (Si113* represent the detected drug-derived from hydrolysis of Pro-Si113-TP - in blue) in (a) A2780-xenografted and (b) non-xenografted female mice model.

VL system (G1946C) (Agilent Technologies, Palo Alto, CA) using a Phenomenex Kinetex C18-100 Å column (150 \times 4.6 mm, 5 μ m particle size) at room temperature. Analyses were carried out with the same chromatographic conditions reported above with a flow rate of 0.6 mL/min and an injection volume of 20 μ L.

3.2.3. Water solubility

Each solid compound (1 mg) was added to 1 mL of distilled water. Each sample was mixed at 20 °C, in a shaker water bath for 24 h [39]. The resulting suspension was filtered through a 0.45 μ m nylon filter (Acrodisc). The concentration of the compound in solution was determined by LC-MS/MS by comparison with the appropriate calibration curve that was obtained from samples of the compound dissolved in methanol at different concentrations. For each compound, the determination was performed in three independent experiments.

3.2.4. Parallel artificial membrane permeability assay (PAMPA)

Each 'donor solution' was prepared from a solution of the appropriate compound (DMSO, 1 mM) diluted with phosphate buffer (pH 7.4, 25.0 mM) up to a final concentration of 500 μ M. The donor wells were filled with 150 μ L of 'donor solution'. The filters were coated with 5 μ L of a solution of phosphatidylcholine in dodecane 1% (w/v) and the lower wells filled with 300 μ L of

'acceptor solution' (50% v/v DMSO and phosphate buffer). The sandwich plate was assembled and incubated for 5 h at room temperature under gentle shaking. After the incubation time, the sandwich was disassembled and the amount of compound in both the donor and acceptor wells was measured by UV/LC-MS. For each compound, the determination was performed in three independent experiments.

Permeability (P_{app}) was calculated according to the following equation obtained from Wohnsland and Faller [40] and Sugano et al. [41] equation with some modification in order to obtain permeability values in cm/s:

$$P_{app} = \frac{V_D \cdot V_A}{(V_D + V_A)At} - \ln(1 - r)$$

where V_A is the volume in the acceptor well (cm^3), V_D is the volume in the donor well (cm^3), A is the "effective area" of the membrane (cm^2), t is the incubation time (s) and r the ratio between drug concentration in the acceptor and equilibrium concentration of the drug in the total volume ($V_D + V_A$). Drug concentration was estimated by using the peak area integration.

Membrane retentions (%MR) were calculated according to the following equation:

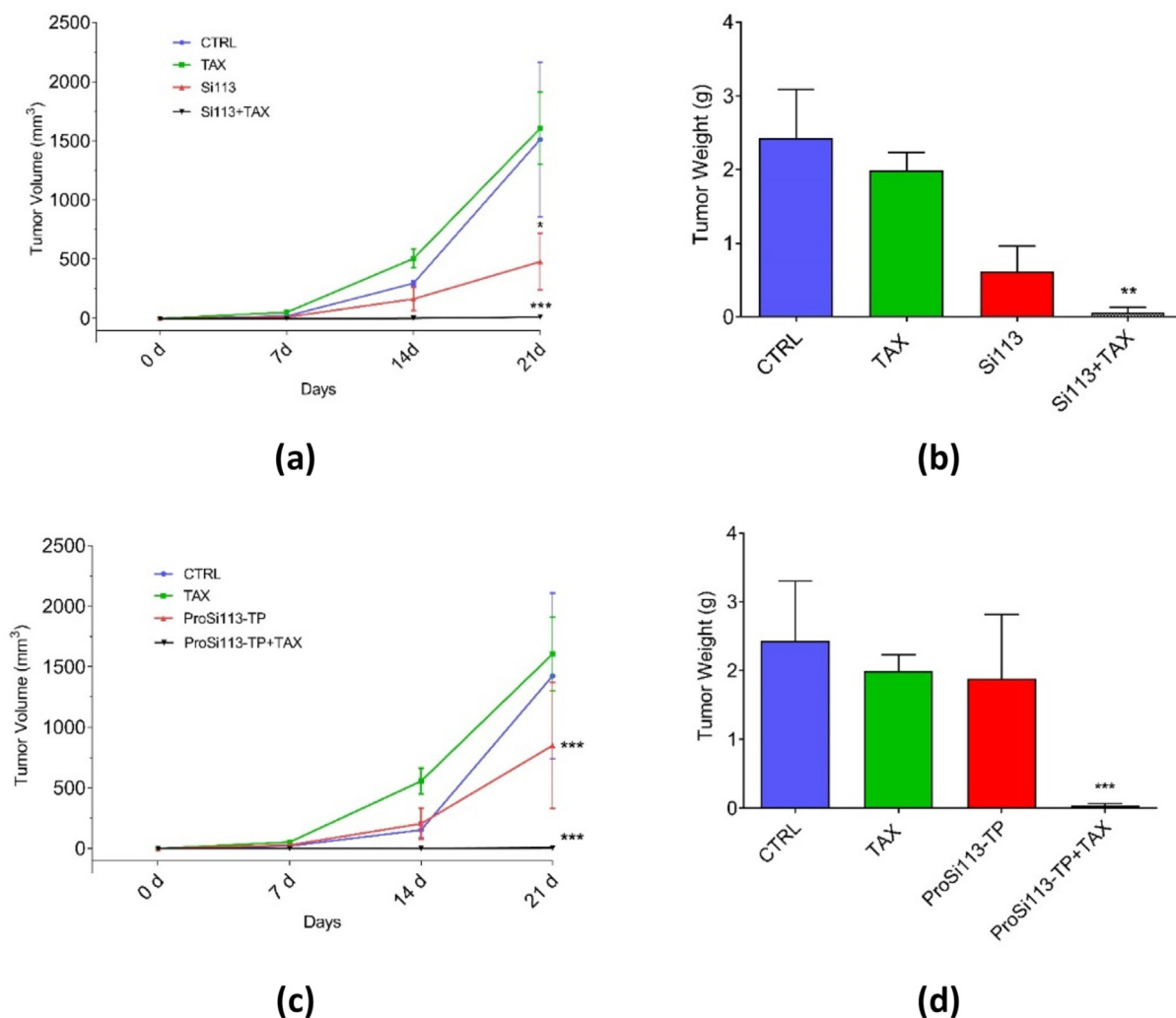


Fig. 10. Ovarian carcinoma *in vivo* efficacy on A2780TC-xenografted mice mode (mean \pm S.D., $n = 5$). Tumor volume after treatment with (a) Paclitaxel (TAX), Si113 and Si113 in combination with TAX and (c) TAX, ProSi113-TP and ProSi113-TP in combination with TAX. Tumor weight after treatment with (b) TAX, Si113 and Si113 in combination with TAX and (d) TAX, ProSi113-TP and ProSi113-TP in combination with TAX. Tumor volume and tumor weight represented in figure (a) and (b) are previously published in D'Antona L. et al. (2019). A Bonferroni's one-way multiple comparisons test (ANOVA) was performed to test the significance of the observed differences. *indicates statistically significant differences between each treatment vs CTRL (* $p < 0.05$, ** $p < 0.01$, *** $p < 0.001$).

$$\%MR = \frac{[r - (D + A)]}{Eq} \cdot 100$$

where r is the ratio between drug concentration in the acceptor and equilibrium concentration, D , A , and Eq represented drug concentration in the donor, acceptor, and equilibrium solution, respectively.

3.2.5. Metabolic stability in HLM (Human liver microsomes)

The incubation mixture (total volume of 500 μ L) was constituted by the following components: human liver microsomes (0.2 mg/mL, 5 μ L), a NADPH regenerating system (NADPH 0.2 mM, NADPH⁺ 1 mM, D-glucose-6-phosphate 4 mM, 4 unit/mL glucose-6-phosphate dehydrogenase and MgCl₂ 48 mM), 50 μ M of each compound in DMSO and phosphate buffer (pH 7.4, 25 mM, up to a final volume of 500 μ L). The mixture was incubated at 37 $^{\circ}$ C for 1 h. The reaction was cooled down and quenched with acetonitrile (1.0 mL). After centrifugation (4000 rpm for 10 min), the supernatant was taken, dried under nitrogen flow, suspended in 100 μ L of methanol and analyzed by UV/LC-MS to determine the percentage of the compound that was not metabolized. For each

compound, the determination was performed in three independent experiments.

3.2.6. Stability tests

3.2.6.1. In polar solvents. Each prodrug was dissolved at r.t. in DMSO, MeOH or Tris-buffer (100 mM, pH 7.4) up to a final concentration of 500 μ M. Aliquot samples (20 μ L) were taken at fixed time points (0.0, 0.25, 0.50, 0.75, 1.0, 2.0, 3.0, 4.0, 5.0, 6.0, 7.0, 8.0, 24.0 and 48 h) and were analyzed by UV/LC-MS. For each compound, the determination was performed in three independent experiments.

3.2.6.2. In human plasma. Pooled human plasma (1.5 mL, 55.7 μ g protein/mL) [42], phosphate buffer (1.4 mL, pH 7.4, 25 mM) and a prodrug dissolved in DMSO (100 μ L, 3.0 mM) were mixed in a test tube that was incubated at 37 $^{\circ}$ C. At set time points (0.0, 0.25, 0.50, 1.0, 3.0, and 24.0 h), samples of 150 μ L were taken, mixed with 600 μ L of cold acetonitrile and centrifuged at 5000 rpm for 15 min [43]. The supernatant was removed and analyzed by UV/LC-MS to monitor the hydrolysis process of the prodrug. For each compound, the determination was performed in three independent experiments.

3.2.6.3. In human plasmin solution. Human plasmin (10 μ L, 150 μ g/mL), Tris-buffer (970 μ L, pH 7.4, 100 mM) and a solution of the prodrug in DMSO (20 μ L, 7.5 mM) were mixed in a test tube and incubated at 37 °C. At set time points (0.0, 0.25, 0.50, 1.0, 3.0, 6.0 and 24.0 h), samples of 50 μ L were taken, mixed with 200 μ L of cold acetonitrile and centrifuged at 5000 rpm for 15 min [34,44]. The supernatant was removed and analyzed by UV/LC-MS to monitor the hydrolysis process of the prodrug. For each compound, the determination was performed in three independent experiments.

3.3. *In vitro* biological assays

3.3.1. Cell cultures

Human HCC cell lines HepG2 and Huh-7 and Ovarian carcinoma cell line A2780, kindly provided by Prof. Ali O. Gure (Bilkent University, Ankara, Turkey), were cultured in DMEM (Life Technologies, Inc., Grand Island, NY) supplemented with 10% fetal bovine serum (FBS), 2 mM L-Glutamine (Invitrogen-Gibco) and 10000 units/mL Penicillin-Streptomycin (Aurogene), respectively. Cells were cultured at 37 °C in a humidified atmosphere of 5% CO₂ and 95% air.

Briefly, for each cell line, 2.5×10^4 cells were seeded in 12-well plates. The day after seeding, compounds dissolved in DMSO were added at increasing concentrations (0.1, 1.0, 10.0 and 100.0 μ M) and incubated for 24, 48 and 72 h at 37 °C in 5% v/v CO₂. To verify if prodrugs could be activated by plasmin, *in vitro* cytotoxicity assays have been also performed in presence of the enzyme. First, 24 h after seeding, our compounds were added by using serum-free DMEM to which plasmin has been added at a final concentration of 0.2 U/well [43]. Then, cells were incubated for 24 h at 37 °C in 5% v/v CO₂. Cell number and viability were evaluated using Z2 Coulter Counter (Beckman Coulter). IC₅₀ was calculated by GraphPad Prism 6.0 software using the best fitting sigmoid curve. For each compound, the determination was performed in triplicate.

3.3.2. *In vitro* evaluation of Sgk1 kinase inhibition

The evaluation of Sgk1 inhibition was carried out following the same analytical procedures: active kinase (Upstate) was incubated in kinase buffer containing ATP (10 μ M), protein kinase A inhibitor (1 mM; Sigma), dithiothreitol (2 mM), [*g*-³²P]ATP (0.02 mCi/sample), tris HCl pH 7.5 (100 mM) in the absence and in presence of Sgk1tide (KKRNRRLSVA) peptide substrate (1 mM) and our compounds at concentration of 0.6 μ M, 3 μ M, 12.5 μ M. The reaction was allowed to occur for 30 min at room temperature, with gentle agitation, prior to stopping with 10 mL of stopping solution (ATP, 1 mM; bovine serum albumin, 2%; HCl, 0.6% w/v). The reaction mix was centrifuged in an Eppendorf microcentrifuge for 10 min at 14,000 rpm. Supernatants (10 μ L) were applied to a 2.1-cm diameter p81 Whatman paper. After drying at room temperature, the filter was washed four times with phosphoric acid (25 mM), once with acetone, and then counted in a scintillation counter to measure the radioactivity incorporated in the substrate peptide.

3.3.3. Inhibition of Sgk1 kinase activity in an intact cell environment

Cell cultures were serum-starved and treated with 12.5 μ M of Si113 and prodrugs for 18 h before stimulation. 1 μ M insulin was added 30 min before lysis [Lysis buffer: 50 mM Tris-HCl, pH 7.4, 0.15 M NaCl, 0.5% IGEPAL, 25 mM NaF, 1 mM DTT, 1 mM Na₃VO₄ plus protease inhibitor cocktail 10 X (Sigma-Aldrich, St. Louis, MO)]. In these experiments, endogenous Sgk1 was immunoprecipitated by means of a Sgk1-specific rabbit polyclonal antibody (#07–315, EMD Millipore). Immunoprecipitates were employed in the kinase assay reaction as described above.

3.4. Animals

Naive BALB/C mice (aged 4–6 weeks, Charles Rivers - Milan, Italy), and female nude mice (aged 4 weeks, ENVIGO - Udine, Italy) were maintained under pathogen-free conditions and given food and water *ad libitum*. The adaption period to the environment was not less than seven days. All the procedures used on animals in this study were approved by Institutional Animal Use and Care Committee at Università degli Studi "Magna Graecia" di Catanzaro and Università degli Studi di Siena and authorized by the Italian Ministry of Health, according to Legislative Decree 116/92, which implemented the European Directive 86/609/EEC on laboratory animal protection in Italy. Methods for all the conducted experiments were performed in accordance with regulations, standards and guidelines of the Animal Use and Care Committee of Università degli Studi "Magna Graecia" di Catanzaro and Università degli Studi di Siena.

3.4.1. *In vivo* administration of Si113 and prodrugs for PK and BD evaluation

For both *in vivo* studies in healthy male mice and nude female mice for PK and preliminary BD studies, Si113 was dissolved in DMSO [37] while its prodrugs were dissolved in saline solution. The compounds were administered intraperitoneally as a single dose of 9.5 and 21 mg/kg in a final volume of 100 μ L for Si113 and its prodrugs, respectively. Healthy male mice, at several time points (0.25, 0.5, 1, 1.5, 2 and 24 h), after drug administration, were treated i.p. with heparin (5000 U/kg) and sacrificed under CO₂. Blood, liver, spleen, lungs, and kidneys were collected. Three animals were used for each time point. Similarly, two groups of nude female mice (two animals for each experimental group), xenografted mice group (2.5×10^6 A2780TC cells subcutaneously) and non-xenografted group, were treated intraperitoneally as a single dose of 9.5 and 21 mg/kg in a final volume of 100 μ L for Si113 and ProSi113-TP. After 24 h, mice were treated i.p. with heparin (5000 U/kg) and sacrificed under CO₂, blood, and organs were collected. The dosage of the prodrugs was chosen to obtain the same molar ratio as Si113 administered at 9.5 mg/kg.

All blood and organ samples were processed, and LC-MS/MS quantitative analyses were performed. Matrix effect %ME (ionization suppression or ionization enhancement) and recovery (%RE) were evaluated (see Supporting Information for more details). The pharmacokinetic parameters were calculated by non-compartmental analysis using PKSolver software [45].

3.4.1.1. Sample preparation. Blood samples were centrifuged at 5000 rpm for 20 min to separate the plasma fraction, which was subsequently collected in a test tube. 1.0 mL of acetonitrile solution containing Si34 [46] (a pyrazolo[3,4-*d*]pyrimidine compound already used as internal standard, IS) at a concentration of 5 μ g/mL was added to each sample to denature protein component. Samples were centrifuged at 5000 rpm for 20 min, and the supernatant was recovered and analyzed by LC-MS/MS. Liver and the other organs were homogenized using a T10 basic ULTRA-TURRAX® homogenizer (Bioclass, Pistoia, Italy); in order to extract the compound from the tissue, acetonitrile IS solution was added (1.5 mL at the concentration of 5 μ g/mL) to 200 mg of tissue, homogenate and then centrifuged at 5000 rpm for 20 min. The supernatant was recovered, filtered and analyzed by LC-MS/MS. The quantification of each compound was performed by reference to the appropriate calibration curve.

3.4.2. *In vivo* efficacy on HCC xenografted mice model

Si113 was dissolved in DMSO [37] while its prodrugs were dissolved in saline solution. The compounds were administered

intraperitoneally into xenografted nude female mice at the dose of 9.5 and 21 mg/kg for Si113 and its prodrugs respectively to obtain the same molar ratio as Si113 administered. At 6 weeks of age, the mice were subcutaneously injected with 2.5×10^6 HepG2 cells suspended in 200 μL of a 1:1 solution containing RPMI without serum and Matrigel™ solution (BD Collaborative Research) in the dorsal posterior-lateral right region. The mice were randomly assigned to four groups of five animals and then administered vehicle alone (DMSO or saline solution), Si113, ProSi113-TP or ProSi113-LKTP for five days/week. The tumor volumes were measured every 7 days using caliper. Specifically, two perpendicular diameters (a = smaller diameter; b = larger diameter) were measured, and the tumor volume was calculated in accordance with formula $V = \pi/6 \times a^2 \times b$. The mice were placed under general anesthesia and sacrificed by vertebral dislocation.

3.4.3. *In vivo* efficacy on ovarian carcinoma xenografted mice model

Paclitaxel was used at a concentration of 5 mg/kg/day, while ProSi113-TP was administered in saline solution at a dosage of 21 mg/kg/day. At 6 weeks of age, the mice were subcutaneously injected with 2.5×10^6 A2780TC cells suspended in 200 μL of a 1:1 solution containing RPMI without serum and Matrigel™ solution (BD Collaborative Research) in the dorsal posterior-lateral right region. The mice were randomly assigned to four groups of five animals and then treated intraperitoneally with vehicle alone (saline solution), ProSi113-TP and ProSi113-TP in association with Paclitaxel for five days/week. The tumor volumes were measured every 7 days using caliper as described above. The mice were placed under general anesthesia and sacrificed by vertebral dislocation.

3.4.4. Statistical analysis

t-test and Bonferroni's Multiple Comparison Test (One-way ANOVA) was performed to evaluate the differences between groups using GraphPad Prism 8 software (San Diego, CA), and differences were considered significant at * $p < 0.05$, ** $p < 0.01$, and *** $p < 0.001$.

4. Discussion and conclusions

Si113, a Sgk1 inhibitor [1] with potent antiproliferative and proapoptotic effect on different cancer cell lines [2,11,21–23], has been selected for prodrugs development to achieve not only an enhancement of its ADME properties, but also an active target system that allows the release of the parent drug locally into the tumor site. In this context, we have synthesized in good yield two plasmin-activated Si113 prodrugs, including a small amino acid sequence D-Ala-Leu-Lys (TP): ProSi113-TP and ProSi113-LKTP. The rationale of this strategy is to exploit the high affinity of TP for a specific reactive site of plasmin [27], a protease recognized as overexpressed in many tumors, including HCC [28] and ovarian cancer [29,30]. ProSi113-TP is composed by the parent drug and TP portion, connected by ester group, while ProSi113-LKTP presents an ester linker elongated with a chain of four carbon atoms between Si113 and TP. Si113-prodrugs have been fully characterized in terms of their *in vitro* ADME properties. The analysis of thermodynamic solubility demonstrated an improved water solubility for both prodrugs in comparison to the respective drug Si113, validating this approach as an excellent strategy to overcome the poor water solubility of the parent drug. Both prodrugs showed a decrease in passive permeability compared to the parent drug; this was predictable given its high hydrophobic nature. In addition, both prodrugs also showed good metabolic stability, as well as Si113. The ability to release the active compound from each prodrug has been confirmed by hydrolysis assays in human plasma and human

plasmin solution where ProSi113-TP, in human plasma, showed a higher percentage of hydrolysis of the drug but a shorter $t_{1/2}$ value than ProSi113-LKTP; the opposite trend is observed in human plasmin solution. Indeed, the presence of a four-carbon linker in ProSi113-LKTP makes the cleavage site more accessible to plasmin (overexpressed in the tumor district), allowing greater hydrolysis and consequent release of the Si113 parent drug. The *in vitro* inhibition activity of Sgk1 was evaluated for Si113 and both prodrugs. As expected, the prodrugs showed pronounced inhibitory activity only at the highest concentration tested, unlike Si113 which showed inhibition of Sgk1 in a dose-dependent manner (inhibition of Sgk1 activity by 75% as early as 0.6 μM increasing to more than 90% at 12.5 μM). It was interesting to note a significant inhibition of Sgk1 by ProSi113-LKTP already at 0.6 μM by 53% and then increasing to 73% at 12.5 μM . In contrast, ProSi113-TP did not show a marked inhibition at 0.6 μM (only 18%) but only at the highest tested concentration of 12.5 μM showed inhibition of Sgk1 activity equal to 80%. Moreover, the inhibition of Sgk1 kinase was evaluated in an intact cell environment with and without insulin stimulation of Sgk1. Si113 and its prodrugs showed similar inhibition of insulin-stimulated Sgk1 activity, thus suggesting that the prodrugs if hydrolyzed in an intact cellular environment, reach the inhibitory activity of Si113. To obtain further clarification on the inhibitory activity of the two prodrugs on Sgk1, a molecular docking study was performed. The results suggest that the presence of a four-carbon atom linker in ProSi113-LKTP allows the moiety of the parent drug to maintain the spatial orientation of Si113. In contrast to ProSi113-TP which, not possessing an elongated spacer, is unable to maintain the spatial orientation of the Si113 parent drug. This may explain the activity of ProSi113-LKTP shown at 0.6 μM on Sgk1 as opposed to ProSi113-TP. Besides, molecular dynamic simulations confirmed the binding mode stability of Si113 in contrast to the two prodrugs, which did not form a stable complex.

The *in vitro* cytotoxicity was evaluated on HCC HepG2 and Huh-7 cell lines. The same trend was observed for Si113 and ProSi113-LKTP after 72 h, where they showed comparable IC_{50} values on both cell lines unlike ProSi113-TP which showed a cytotoxic effect 3- and almost 14-fold lower than the parent drug and Si113-LKTP on HepG2 and Huh-7 cell lines, respectively. Cytotoxic activity was also evaluated after 24 h in the presence of human plasmin. HepG2 and Huh-7 cells treated in presence of plasmin with ProSi113-TP showed IC_{50} values 2- and 3-fold lower than cells treated without plasmin. In contrast, ProSi113-LKTP showed an increased cytotoxic effect 4-fold higher on HepG2 cell line in presence of plasmin, but similar IC_{50} values on Huh-7 were obtained. The same evaluations were conducted on the ovarian carcinoma A2780 cell line obtaining comparable IC_{50} values after 72 h for Si113 and both prodrugs. On the other hand, in presence of human plasmin, ProSi113-TP showed increased anticancer activity compared to cells treated without plasmin. To complete the pre-clinical profile of Si113 and its prodrugs, *in vivo* pharmacokinetic properties were evaluated in healthy male mice treated intraperitoneally at a dosage of 9.5 and 21 mg/kg for Si113 and prodrugs, respectively. Following administration, Si113 was rapidly detected showing C_{max} of 46.27 nmol/mL while the observed C_{max} for ProSi113-TP and ProSi113-LKTP was 8.09 and 2.66 nmol/mL, respectively. Moreover, the Si113 obtained from hydrolysis of ProSi113-LKTP showed a C_{max} value 4-fold higher than Si113 released from the ProSi113-TP prodrug.

The plasma half-life remains in the same range after treatment with ProSi113-TP (15.30 h) and ProSi113-LKTP (21.82 h). On the other hand, Si113 showed a $t_{1/2}$ value more than 5-fold lower than its prodrugs. Si113 and its prodrugs were detected in all tissues analyzed at 24 h after administration. ProSi113-LKTP showed a higher tissue concentration than Si113 and ProSi113-TP in hepatic

tissue and the same trend is observed in kidneys, lungs, and splenic tissue. Starting from the *in vitro* activity profile, ProSi113-TP was selected for a preliminary 24 h biodistribution study in female nude mice. The test was conducted to assess drug uptake in the ovaries and tumor mass. In two groups of animals, A2780-xenografted and non-xenografted mice, in ovaries, ProSi113-TP was found 2-fold higher than Si113 (4.11 and 1.89 nmol/g, respectively) and the same trend is observed in the ovaries of non-xenografted mice. Moreover, higher concentrations of ProSi113-TP were detected in the tumor mass (5.69 nmol/g). In contrast, the parental drug Si113 showed almost 3-fold lower tissue concentration (2.20 nmol/g) than its prodrug. Finally, their antitumor efficacy was evaluated in HCC and ovarian carcinoma mice models. In HCC murine model, an impressive reduction in tumor growth was recorded in all treated compared to control with a reduction in tumor weight of around 90%. Concerning the antitumor effectiveness on the paclitaxel-resistant ovarian carcinoma mouse model, as expected, treatment with paclitaxel had no effect on tumor growth. The same was achieved following treatment with ProSi113-TP alone, which showed no significant reduction compared to paclitaxel treatment, but a substantial reduction in tumor volume was obtained when it is used in combination with paclitaxel resulting in a reduction in tumor mass weight of approximately 85% compared to control.

In conclusion, the results confirmed not only the promising antitumor action of Si113 already widely studied, but also a valid active target strategy through a prodrug approach, able to improve the uptake in cancer cells and not less, improve the pharmacokinetic properties of the parent drug suffering to low water solubility. This has made it possible to obtain prodrugs that can be formulated in aqueous solutions, more manageable, and well-tolerated *in vivo* by systemic route. Therefore, we believe that the developed prodrugs, especially ProSi113-TP, given its remarkable *in vivo* antitumor activity on HCC and especially in association with paclitaxel on paclitaxel-resistant ovarian carcinoma, a promising alternative to the common chemotherapeutic agents. For this reason, through further studies and investigations, these compounds could be the subject of future clinical trials.

Funding

E.R., E.D. and M.B. were supported by AIRC (Associazione Italiana per la Ricerca sul Cancro, Italy) Grant IG-2015, code 17677.

Author contribution

The authors Enrico Rango and Lucia D'Antona contributed equally to this work. Conceptualization: G.I., A.B., A.Mo. and A.L.F.; design and synthesis of Si113 and prodrugs: G.I., A.B., A.Mo. and A.C.; enzymatic study's methodology: L.D. and N.P.; *in vitro* ADME studies: E.R., G.I., and S.M.; *in silico* studies: C.I.T.; cell cytotoxicity study's methodology: C.Z. and A.L.F.; *in vivo* PK study's methodology: E.R., A.Ma., and C.Z.; *in vivo* efficacy study's methodology: L.D. and N.P.; validation: E.R., A.Ma., G.I., A.Mo. and C.Z.; formal analysis: E.R., A.Ma. and G.I.; resources: N.P., S.S., E.D. and M.B.; data curation: E.R. and L.D.; writing -original draft preparation: E.R., L.D. and A.Ma.; writing -review and editing: E.R., L.D., A.B., N.P. and E.D.; supervision: S.S., N.P. and E.D.; project administration: S.S., N.P., E.D. and M.B.; funding acquisition: S.S., E.D. and M.B.

Conflicts of interest

All authors have no competing interests.

Declaration of competing interest

The authors declare that they have no known competing financial interests or personal relationships that could have appeared to influence the work reported in this paper.

Acknowledgments

This manuscript was realized in memory of Maurizio Botta, deceased on August 2, 2019.

Appendix A. Supplementary data

Supplementary data to this article can be found online at <https://doi.org/10.1016/j.ejmech.2021.113653>.

References

- [1] F. Ortuso, R. Amato, A. Artese, L. D'antona, G. Costa, C. Talarico, F. Gigliotti, C. Bianco, F. Trapasso, S. Schenone, F. Musumeci, L. Botta, N. Perrotti, S. Alcaro, Silico identification and biological evaluation of novel selective serum/glucocorticoid-inducible kinase 1 inhibitors based on the pyrazolo-pyrimidine scaffold, *J. Chem. Inf. Model.* 54 (2014) 1828–1832, <https://doi.org/10.1021/ci500235f>.
- [2] L. D'Antona, R. Amato, C. Talarico, F. Ortuso, M. Menniti, V. Dattilo, R. Iuliano, F. Gigliotti, A. Artese, G. Costa, S. Schenone, F. Musumeci, C. Abbruzzese, L. Botta, F. Trapasso, S. Alcaro, M.G. Paggi, N. Perrotti, SI113, a specific inhibitor of the Sgk1 kinase activity that counteracts cancer cell proliferation, *Cell. Physiol. Biochem.* 35 (2015) 2006–2018, <https://doi.org/10.1159/000374008>.
- [3] Y. Sang, P. Kong, S. Zhang, L. Zhang, Y. Cao, X. Duan, T. Sun, Z. Tao, W. Liu, SGK1 in human cancer: emerging roles and mechanisms, *Front. Oncol.* 10 (2021), <https://doi.org/10.3389/fonc.2020.608722>, 2987.
- [4] B.A. Hall, T.Y. Kim, M.N. Skor, S.D. Conzen, Serum and glucocorticoid-regulated kinase 1 (SGK1) activation in breast cancer: requirement for mTORC1 activity associates with ER- α expression, *Breast Cancer Res. Treat.* 135 (2012) 469–479, <https://doi.org/10.1007/s10549-012-2161-y>.
- [5] E.M. Sommer, H. Dry, D. Cross, S. Guichard, B.R. Davies, D.R. Alessi, Elevated SGK1 predicts resistance of breast cancer cells to Akt inhibitors, *Biochem. J.* 452 (2013) 499–508, <https://doi.org/10.1042/BJ20130342>.
- [6] M. Isikbay, K. Otto, S. Kregel, J. Kach, Y. Cai, D.J. Vander Griend, S.D. Conzen, R.Z. Szmulewitz, Glucocorticoid receptor activity contributes to resistance to androgen-targeted therapy in prostate cancer, *Hormones Canc.* 5 (2014) 72–89, <https://doi.org/10.1007/s12672-014-0173-2>.
- [7] E.M. Stringer-Reasor, G.M. Baker, M.N. Skor, M. Kocherginsky, E. Lengyel, G.F. Fleming, S.D. Conzen, Glucocorticoid receptor activation inhibits chemotherapy-induced cell death in high-grade serous ovarian carcinoma, *Gynecol. Oncol.* 138 (2015) 656–662, <https://doi.org/10.1016/j.ygyno.2015.06.033>.
- [8] C. Abbruzzese, S. Mattarocci, L. Pizzuti, A.M. Mileo, P. Visca, B. Antoniani, G. Alessandrini, F. Facciolo, R. Amato, L. D'Antona, M. Rinaldi, A. Felsani, N. Perrotti, M.G. Paggi, Determination of SGK1 mRNA in non-small cell lung cancer samples underlines high expression in squamous cell carcinomas, *J. Exp. Clin. Oncol. Res.: CR (Clim. Res.)* 31 (2012), <https://doi.org/10.1186/1756-9966-31-4>, 4.
- [9] E.J. Chung, Y.K. Sung, M. Farooq, Y. Kim, S. Im, W.Y. Tak, Y.J. Hwang, Y. Il Kim, H.S. Han, J.-C. Kim, M.K. Kim, Gene expression profile analysis in human hepatocellular carcinoma by cDNA microarray, *Mol. Cell.* 14 (2002) 382–387.
- [10] M. Won, K.A. Park, H.S. Byun, Y.-R. Kim, B.L. Choi, J.H. Hong, J. Park, J.H. Seok, Y.-H. Lee, C.-H. Cho, I.S. Song, Y.K. Kim, H.-M. Shen, G.M. Hur, Protein kinase SGK1 enhances MEK/ERK complex formation through the phosphorylation of ERK2: implication for the positive regulatory role of SGK1 on the ERK function during liver regeneration, *J. Hepatol.* 51 (2009) 67–76, <https://doi.org/10.1016/j.jhep.2009.02.027>.
- [11] C. Talarico, V. Dattilo, L. D'Antona, A. Barone, N. Amodio, S. Belviso, F. Musumeci, C. Abbruzzese, C. Bianco, F. Trapasso, S. Schenone, S. Alcaro, F. Ortuso, T. Florio, M.G. Paggi, N. Perrotti, R. Amato, SI113, a SGK1 inhibitor, potentiates the effects of radiotherapy, modulates the response to oxidative stress and induces cytotoxic autophagy in human glioblastoma multiforme cells, *Oncotarget* 7 (2016) 15868–15884, <https://doi.org/10.18632/oncotarget.7520>.
- [12] N. Perrotti, R.A. He, S.A. Phillips, C.R. Haft, S.I. Taylor, Activation of serum- and glucocorticoid-induced protein kinase (sgk) by cyclic AMP and insulin, *J. Biol. Chem.* 276 (2001) 9406–9412, <https://doi.org/10.1074/jbc.M007052200>.
- [13] M. Föller, D.S. Kempe, K.M. Boini, G. Pathare, B. Siraskar, P. Capuano, I. Alesutan, M. Sopiani, G. Stange, N. Mohebbi, M. Bhandaru, T.F. Ackermann, M.S. Judenhofer, B.J. Pichler, J. Biber, C.A. Wagner, F. Lang, PKB/SGK-resistant GSK3 enhances phosphaturia and calciuria, *J. Am. Soc. Nephrol.* 22 (2011) 873–880, <https://doi.org/10.1681/ASN.2010070757>.
- [14] F. Lang, J. Voelkl, Therapeutic potential of serum and glucocorticoid inducible

- kinase inhibition, *Expet Opin. Invest. Drugs* 22 (2013) 701–714, <https://doi.org/10.1517/13543784.2013.778971>.
- [15] S.Y. Chen, A. Bhargava, L. Mastroberardino, O.C. Meijer, J. Wang, P. Buse, G.L. Firestone, F. Verrey, D. Pearce, Epithelial sodium channel regulated by aldosterone-induced protein sgk, *Proc. Natl. Acad. Sci. U. S. A* 96 (1999) 2514–2519, <https://doi.org/10.1073/pnas.96.5.2514>.
- [16] P. Castel, H. Ellis, R. Bago, E. Toska, P. Razavi, F.J. Carmona, S. Kannan, C.S. Verma, M. Dickler, S. Chandrapaty, E. Brogi, D.R. Alessi, J. Baselga, M. Scaltriti, PDK1-SGK1 signaling sustains AKT-independent mTORC1 activation and confers resistance to PI3K inhibition, *Canc. Cell* 30 (2016) 229–242, <https://doi.org/10.1016/j.ccell.2016.06.004>.
- [17] A. Oriacchio, M. Ranieri, M. Brave, V.A. Arciuch, T. Forde, D. De Martino, K.E. Anderson, P. Hawkins, A. Di Cristofano, SGK1 is a critical component of an AKT-independent pathway essential for PI3K-mediated tumor development and maintenance, *Canc. Res.* 77 (2017) 6914–6926, <https://doi.org/10.1158/0008-5472.CAN-17-2105>.
- [18] F. Lang, E. Shumilina, Regulation of ion channels by the serum- and glucocorticoid-inducible kinase SGK1, *FASEB (Fed. Am. Soc. Exp. Biol.) J.* 27 (2013) 3–12, <https://doi.org/10.1096/fj.12-218230>.
- [19] R. Amato, L. D'Antona, G. Porciatti, V. Agosti, M. Menniti, C. Rinaldo, N. Costa, E. Bellacchio, S. Mattarocci, G. Fuiano, S. Soddu, M.G. Paggi, F. Lang, N. Perrotti, Sgk1 activates MDM2-dependent p53 degradation and affects cell proliferation, survival, and differentiation, *J. Mol. Med.* 87 (2009) 1221–1239, <https://doi.org/10.1007/s00109-009-0525-5>.
- [20] R. Amato, D. Scumaci, L. D'Antona, R. Iuliano, M. Menniti, M. Di Sanzo, M.C. Faniello, E. Colao, P. Malatesta, A. Zingone, V. Agosti, F.S. Costanzo, A.M. Mileo, M.G. Paggi, F. Lang, G. Cuda, P. Lavia, N. Perrotti, Sgk1 enhances RANBP1 transcript levels and decreases taxol sensitivity in RKO colon carcinoma cells, *Oncogene* 32 (2013) 4572–4578, <https://doi.org/10.1038/onc.2012.470>.
- [21] C. Talarico, L. D'Antona, D. Scumaci, A. Barone, F. Gigliotti, C.V. Fiumara, V. Dattilo, E. Gallo, P. Visca, F. Ortuso, C. Abbruzzese, L. Botta, S. Schenone, G. Cuda, S. Alcaro, C. Bianco, P. Lavia, M.G. Paggi, N. Perrotti, R. Amato, Preclinical model in HCC: the SGK1 kinase inhibitor SI113 blocks tumor progression in vitro and in vivo and synergizes with radiotherapy, *Oncotarget* 6 (2015) 37511–37525, <https://doi.org/10.18632/oncotarget.5527>.
- [22] L. D'Antona, V. Dattilo, G. Catalogna, D. Scumaci, C.V. Fiumara, F. Musumeci, G. Perrotti, S. Schenone, R. Talerico, C.B. Spoletti, N. Costa, R. Iuliano, G. Cuda, R. Amato, N. Perrotti, In Preclinical model of ovarian cancer, the SGK1 inhibitor SI113 counteracts the development of paclitaxel resistance and restores drug sensitivity, *Transl. Oncol.* 12 (2019) 1045–1055, <https://doi.org/10.1016/j.tranon.2019.05.008>.
- [23] D. Conza, P. Mirra, G. Cali, T. Tortora, L. Insabato, F. Fiory, S. Schenone, R. Amato, F. Beguinot, N. Perrotti, L. Ulianich, The SGK1 inhibitor SI113 induces autophagy, apoptosis, and endoplasmic reticulum stress in endometrial cancer cells, *J. Cell. Physiol.* 232 (2017) 3735–3743, <https://doi.org/10.1002/jcp.25850>.
- [24] K.J. Yoon, P.M. Potter, M.K. Danks, Development of prodrugs for enzyme-mediated, tumor-selective therapy, *Curr. Med. Chem. Anti Canc. Agents* 5 (2005) 107–113, <https://doi.org/10.2174/1568011053174837>.
- [25] I. Giang, E.L. Boland, G.M.K. Poon, Prodrug applications for targeted cancer therapy, *AAPS J.* 16 (2014) 899–913, <https://doi.org/10.1208/s12248-014-9638-z>.
- [26] X. Zhang, X. Li, Q. You, X. Zhang, Prodrug strategy for cancer cell-specific targeting: a recent overview, *Eur. J. Med. Chem.* 139 (2017) 542–563, <https://doi.org/10.1016/j.ejmech.2017.08.010>.
- [27] P.K. Chakravarty, P.L. Carl, M.J. Weber, J.A. Katzenellenbogen, Plasmin-activated prodrugs for cancer chemotherapy. 2. Synthesis and biological activity of peptidyl derivatives of doxorubicin, *J. Med. Chem.* 26 (1983) 638–644, <https://doi.org/10.1021/jm00359a004>.
- [28] Q. Zheng, Z.Y. Tang, Q. Xue, D.R. Shi, H.Y. Song, H.B. Tang, Invasion and metastasis of hepatocellular carcinoma in relation to urokinase-type plasminogen activator, its receptor and inhibitor, *J. Canc. Res. Clin. Oncol.* 126 (2000) 641–646, <https://doi.org/10.1007/s004320000146>.
- [29] E. Pujade-Lauraine, H. Lu, S. Mirshahi, J. Soria, C. Soria, A. Bernadou, E.K.O. Kruthof, H.R. Lijnen, P. Burtin, The plasminogen-activation system in ovarian tumors, *Int. J. Canc.* 55 (1993) 27–31, <https://doi.org/10.1002/ijc.2910550106>.
- [30] G. Konecny, M. Untch, A. Pihan, R. Kimmig, M. Gropp, P. Stieber, H. Hepp, D. Slamon, M. Pegram, Association of urokinase-type plasminogen activator and its inhibitor with disease progression and prognosis in ovarian cancer, *Clin. Canc. Res.* 7 (2001) 1743–1749.
- [31] H.C. Kwaan, B. McMahon, The role of plasminogen-plasmin system in cancer, *Canc. Treat Res.* 148 (2009) 43–66, https://doi.org/10.1007/978-0-387-79962-9_4.
- [32] O. Saksela, D.B. Rifkin, Cell-associated plasminogen activation: regulation and physiological functions, *Annu. Rev. Cell Biol.* 4 (1988) 93–126, <https://doi.org/10.1146/annurev.cellbio.4.1.93>.
- [33] L. Devy, F.M.H. de Groot, S. Blacher, A. Hajitou, P.H. Beusker, H.W. Scheeren, J.M. Foidart, A. Noël, Plasmin-activated doxorubicin prodrugs containing a spacer reduce tumor growth and angiogenesis without systemic toxicity, *Faseb. J.: Off. Publ. Feder. Am. Soc. Exper. Biol.* 18 (2004) 565–567, <https://doi.org/10.1096/fj.03-0462fj>.
- [34] F.M.H. De Groot, L.W.A. Van Berkum, H.W. Scheeren, Synthesis and biological evaluation of 2'-carbamate-linked and 2'-carbonate-linked prodrugs of paclitaxel selective activation by the tumor-associated protease plasmin, *J. Med. Chem.* 43 (2000) 3093–3102, <https://doi.org/10.1021/jm0009078>.
- [35] P. Calandro, G. Iovenitti, C. Zamperini, F. Candita, E. Dreassi, M. Chiariello, A. Angelucci, S. Schenone, M. Botta, A. Mancini, Plasmin-binding tripeptide-decorated liposomes loading pyrazolo[3,4-d]pyrimidines for targeting hepatocellular carcinoma, *ACS Med. Chem. Lett.* 9 (2018) 646–651, <https://doi.org/10.1021/acsmchemlett.8b00062>.
- [36] M. Radi, E. Dreassi, C. Brullo, E. Crespan, C. Tintori, V. Bernardo, M. Valoti, C. Zamperini, H. Daigl, F. Musumeci, F. Carraro, A. Naldini, I. Filippi, G. Maga, S. Schenone, M. Botta, Design, synthesis, biological activity, and ADME properties of pyrazolo[3,4-d]pyrimidines active in hypoxic human leukemia Cells: a lead optimization study, *J. Med. Chem.* 54 (2011) 2610–2626, <https://doi.org/10.1021/jm1012819>.
- [37] T. Kelava, I. Čavar, F. Culo, Influence of small doses of various drug vehicles on acetaminophen-induced liver injury, *Can. J. Physiol. Pharmacol.* 88 (2010) 960–967, <https://doi.org/10.1139/Y10-065>.
- [38] M. Radi, C. Tintori, F. Musumeci, C. Brullo, C. Zamperini, E. Dreassi, A.L. Fallacara, G. Vignaroli, E. Crespan, S. Zanoli, I. Laurenzana, I. Filippi, G. Maga, S. Schenone, A. Angelucci, M. Botta, Design, synthesis, and biological evaluation of pyrazolo[3,4-d]pyrimidines active in vivo on the Bcr-Abl T3151 mutant, *J. Med. Chem.* 56 (2013) 5382–5394, <https://doi.org/10.1021/jm400233w>.
- [39] B. Bard, S. Martel, P.A. Carrupt, High throughput UV method for the estimation of thermodynamic solubility and the determination of the solubility in bio-relevant media, *Eur. J. Pharmaceut. Sci.* 33 (2008) 230–240, <https://doi.org/10.1016/j.ejps.2007.12.002>.
- [40] F. Wohnsland, B. Faller, High-throughput permeability pH profile and high-throughput alkane/water log P with artificial membranes, *J. Med. Chem.* 44 (2001) 923–930, <https://doi.org/10.1021/jm001020e>.
- [41] K. Sugano, H. Hamada, M. Machida, H. Ushio, High throughput prediction of oral absorption: improvement of the composition of the lipid solution used in parallel artificial membrane permeation assay, *J. Biomol. Screen* 6 (2001) 189–196, <https://doi.org/10.1177/108705710100600309>.
- [42] M. Bradford, A rapid and sensitive method for the quantitation of microgram quantities of protein utilizing the principle of protein-dye binding, *Anal. Biochem.* 72 (1976) 248–254, <https://doi.org/10.1006/abio.1976.9999>.
- [43] B.L. Barthel, D.L. Rudnicki, T.P. Kirby, S.M. Colvin, D.J. Burkhart, T.H. Koch, Synthesis and biological characterization of protease-activated prodrugs of doxazolidine, *J. Med. Chem.* 55 (2012) 6595–6607, <https://doi.org/10.1021/jm300714p>.
- [44] F.M.H. De Groot, H.J. Broxterman, H.P.H.M. Adams, A. Van Vliet, G.I. Tesser, Y.W. Elderkamp, A.J. Schraa, R.J. Kok, G. Molema, H.M. Pinedo, H.W. Scheeren, Design, synthesis, and biological evaluation of a dual tumor-specific motive containing integrin-targeted plasmin-cleavable doxorubicin prodrug, *Mol. Canc. Therapeut.* 1 (2002) 901–911.
- [45] Y. Zhang, M. Huo, J. Zhou, S. Xie, PKSolver: an add-in program for pharmacokinetic and pharmacodynamic data analysis in Microsoft Excel, *Comput. Methods Progr. Biomed.* 99 (2010) 306–314, <https://doi.org/10.1016/j.cmpb.2010.01.007>.
- [46] A.L. Fallacara, C. Zamperini, A. Podolski-Renić, J. Dinić, T. Stanković, M. Stepanović, A. Mancini, E. Rango, G. Iovenitti, A. Molinari, F. Bugli, M. Sanguinetti, R. Torelli, M. Martini, L. Maccari, M. Valoti, E. Dreassi, M. Botta, M. Pešić, S. Schenone, A new strategy for glioblastoma treatment: in vitro and in vivo preclinical characterization of SI306, a pyrazolo[3,4-d]pyrimidine dual Src/P-Glycoprotein inhibitor, *Cancers* 11 (2019), <https://doi.org/10.3390/cancers11060848>.